Optimization of multi-wavelength Photoplethysmographic for wearable heart rate acquisition

Weiqing Huang

School of Science

Master Thesis of Master's Programme in ICT Innovation.
Espoo 23.4.2018

Thesis supervisor:

Vesa Hirvisalo
Senior university lecturer

Thesis advisor:

Ilkka Korhonen, PhD

Aalto University
School of Science

AALTO UNIVERSITY
SCHOOL OF SCIENCE

ABSTRACT OF THE
MASTER'S THESIS

Author: Weiqing Huang

Title: Optimization of multi-wavelength Photoplethysmographic for wearable heart rate acquisition

Date: 23.4.2018 Language: English Number of pages: 6+49

Department of Science

Professorship: Master's programme in ICT Innovation - Embedded Systems

Supervisor: Vesa Hirvisalo
Senior university lecturer
Advisor: Ilkka Korhonen, PhD

Photoplethysmographic is an optical measure technique for heart rate monitoring on the surface of the skin. PPG based wearable heart rate monitor has become popular in consumer targeted market. This thesis work is based on the PulseOn product development and the final implementation will be integrated into the PulseOn OHRM sensor product.

Choice of the wavelength of PPG is a trade-off between power consumption and accuracy considering the activity type, skin color and skin perfusion. The subject of this thesis is implementing a channel selection algorithm, which is green and IR channel, on a commercially available PulseOn wrist band to optimize the power consumption and accuracy of the measurement. The channel selection algorithm is first implemented and evaluated in Matlab simulation and then implemented in C code.

Performance of the channel selection algorithm on the device is evaluated considering various factors, including skin color, tightness of the wristband. The results show that channel selection algorithm can not only reduce the power consumption but also help to handle the measurement on different measurement conditions.

Keywords: Photoplethysmographic; Wearable heart rate monitor; Channel selection algorithm

Preface

I want to thank my supervisor Vesa Hirvisalo and instructor Ilkka Korhonen for their guidance.Also, I want to thank my college Marko Nurmi and Tuomas Halkola for their supports during the thesis work period.

Thanks my families for their loves and supports for all these years. I cannot achieve this without them. I want to thanks my friend, Xin Yu, for the check and modification suggestion of this thesis.

Thanks Yixuan Zheng for the remote supports during the period of writing the thesis. May the force be with her and all the best with her thesis.

Wish my dear sister: happy wedding, sweet love, a happy marriage.

Otaniemi, 23.04.2018

Weiqing Huang

Contents

Abbreviations

AC	alternating current
ADC	analog-to-digital convert
DAC	digital-to-analog converter
DC	direct current
ECG	electrocardiogram
H2O	water
Hb	hemoglobin
HbO2	oxyhemoglobin
HR	heart rate
HRV	heart rate variability
IBI	inter-beat-interval
IR	infrared
LED	light-emitting diode
MAE	mean absolute error
MCU	microcontroller
O2	oxygen
OHRM	optical heart rate monitoring
PPG	photoplethysmography
SNR	signal-to-noise ratio
TIA	transimpedance amplifier

1 Introduction

Heart rate monitoring has been applied widely in clinical studies for the prediction of diabetic neuropathy and cardiological diseases. Additionally, it is popular to use HR monitor to report oxygen uptake and energy expenditure of the athletes to optimize the training. As consumer's interest in health and fitness increase rapidly, wearable heart rate monitor, especially based on photoplethysmographic (PPG), has become a focus in this field.

1.1 Research problem

Photoplethysmography(PPG) is an optical measure technique that can be implemented to detect blood volume changes in the microvascular bed of tissue. It has a common application currently, including sports monitoring, pulse oximeters, digital beat-to-beat blood pressure measurement systems. Only a few optoelectronic components are required to implement PPG technology: a light source to illuminate the measured tissue and a photodetector to sample the variations in light intensity generated by the change of blood volume. PPG is mostly utilized non-invasively and operate at a green or a near infrared wavelength to get a better quality signal.

Although the principle of PPG sensing is straightforward, wrist based optical heart rate monitoring in consumer applications poses a challenge for PPG sensor design. The signal of interest is typically 0.1 – 1 % of the surrounding component with signal-to-noise ratio (SNR) of around 20 dB [1][2]. Addition of motion and ambient light artifacts from daily life and sports may drop the SNR to -20 dB and below [3][4]. The poor SNR sets strict requirements for the signal acquisition analog front end(AFE) specifically regarding noise performance and dynamic range. Additionally, wrist-worn devices often have very small batteries, which makes power consumption one of the main limitations [5]. These problems have been solved by Nurmi in his thesis by developing an embedded control algorithm that runs on a consumer-targeted optical heart rate monitoring wrist device and optimally adjusts the parameters of the PPG front end in the PulseOn P-OHR1F module.

The choice of wavelength of the light source is a balance between the signal quality and power consumption considering its application scenarios. The reflected green light is usually selected as the light source in normal ambient temperature with light skin color for its better AC/DC component ratio of the PPG signal. However, reflected IR light could be desirable when reaching deeper tissue is needed in cold ambient temperature or dark skin conditions. In addition, the power consumption of IR light is less than that of green light.

Based on Nurmi's work [5], the objective of this thesis is to implement the multi-wavelength(especially green and IR) control logic for selecting and switching channels on PulseOn OHRM wrist device using AFE 4404. The goals of channel selection are increasing the accuracy of HR estimation and reducing power consumption.

1.2 Thesis contribution

This thesis first simulates a channel selection algorithm in Matlab and then implements on PulseOn OHRM device. The experiments of effect of skin color and tightness level on the performance of channel selection algorithm were conducted and the results are presented in section 6. The work by the author consisted of:

- Matlab simulation and algorithm improvement of channel selection based on the simulation result.
- Implementation of channel switching between green and IR channel, as well as testing and debugging on PulseOn device.
- Modify raw data processing script and introduce script for auto-testing.
- Evaluation of the effect of skin color and tightness of the device on the performance of channel selection implementation.

1.3 Structure of the thesis

The organization of this thesis paper is shown below:

- Section 1 presents the problems, objectives and the contribution of this thesis.
- Section 2 provides the background, including the introduction of PPG technique, applications of optical heart rate monitoring device and factors that affect the quality of PPG signal.
- Section 3 shows the signal chain of typical front end and important signal process modules, as well as the parameters related to range enhancement.
- Section 4 introduces the PulseOn OHRM device and its AFE4404 module. This section also offers the description of methods related to the data collection process.
- Section 5 provides the introduction of the channel selection algorithm and shows the details of simulation in Matlab and implementation on the device.
- Section 6 presents the results from simulations and tests on the device, together with the analysis of the results.
- Section 7 summarizes this thesis work and gives a future plan.

2 Background

2.1 Photoplethysmography(PPG)

The principle of PPG technology is an optical detection of blood volume changes in the microvascular bed of tissue with a light source and photodetector. The PPG sensor gets information of small variations in blood perfusion of the tissue and pulse rate through monitoring the light intensity of transmission through or reflection from the tissue.

2.1.1 PPG wave

Each heart beat generates a blood pressure pulse which will propagate in the blood vessel. A local increase of the blood pressure will modify both the properties and the geometry of the blood vessel due to the changes of volume and blood composition and concentration, respectively. This increases the light absorption and causes an attenuation of the transmitted light intensity. The property changes of blood vessel result in the variation of the observed PPG signal.

A typical PPG signal consists of direct current(DC) and alternating current(AC) components as shown in Figure 1. DC components correspond to the non-pulsatile average detected optical signal while AC corresponds to the time-varying pulsatile light signal. The non-pulsatile component results from light absorption due to venous blood, tissue, and diastolic volume of the arterial blood [6]. The AC component indicates variation in the blood volume that occurs between the diastolic and systolic phases of the cardiac cycle; the major frequency of the AC component depends on the heart rate and is add on the DC component [7].

2.1.2 Measurement configuration

The transmitted light captured by the photodetector may come from two different modes, as displayed in Figure 2.

In a transmission mode, the light transmitted through the tissue is gathered by a photodetector opposite the light source, while in reflectance mode, the photodetector is placed next to the light source onto the skin surface and detects the reflected and back-scattered from the tissue and blood vessels.

A better signal might be obtained through transmission mode, however, only the sites where transmitted light can go through can be applied with this mode, such as fingertip, nasal septum, cheek, tongue, earlobe. While Performing the PPG analysis at body locations such as the the ankle, the sternum, or forehead, the emitted light is absorbed before reaching the opposite side of the body [6]. In these cases, reflectance mode, an alternative configuration, can eliminate the problem associated with sensor placement.

The reflectance mode has the benefit of performing the PPG measurement on any skin area theoretically, however, the measured PPG signal is commonly smaller and affected by pressure disturbances and motion artifacts. All the movements, such as physical activity, might generate motion artifacts that disturb the PPG signal and

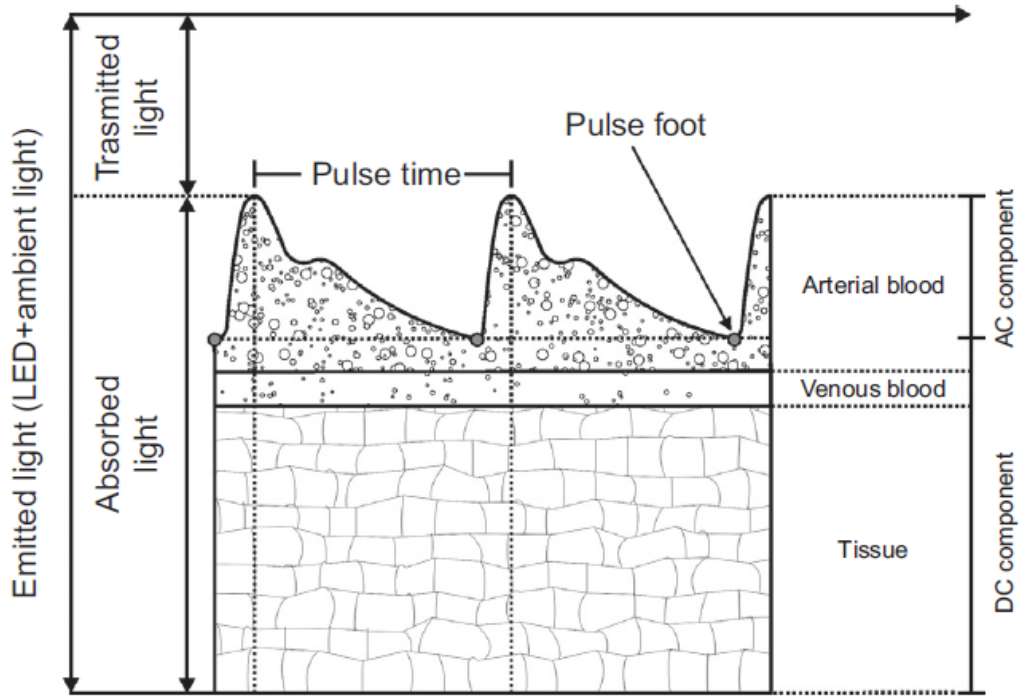

Figure 1: Simplified representation the DC and AC components of PPG signal[6].

limit the measurement accuracy of physiological parameters. Pressure disturbances acting upon the probe can disfigure the arterial geometry by compression. Therefore, in the reflected PPG signal,the pressure on the skin can influence the AC amplitude [7].

2.1.3 Wavelength

The wavelength of the light source plays an important role in the interaction of light and tissues. When a precise wavelength light travels through the tissue, each tissue constituent reveals a specific optical behavior. The specific optical behavior can be presented as the absorption spectrum in Figure 3 considering the coefficient of absorption of a specific molecule concerning the light wavelength.

The absorption spectrum of main constituent tissue, water (H2O), shows that transmission of wavelengths shorter than 950 nm is more efficient. Light wavelengths shorter than 500 nm will be strongly absorbed by another constituent, Melanin. The skin concentration of Melanin is depended on the skin pigmentation [6]. Hemoglobin (Hb) is a dominant component of blood, whose absorbing characteristics vary with its chemical binding. Hb molecules which cannot bind reversibly with molecular oxygen are called dysfunctional hemoglobin (e.g., methemoglobin, carboxyhemoglobin, and sulfhemoglobin). Functional hemoglobin is called reduced Hb if it is not fully saturated with oxygen (i.e., carrying four O2 molecules) and oxyhemoglobin (HbO2) if it is fully saturated. Most of the Hb molecules are of the functional type in healthy persons [6].

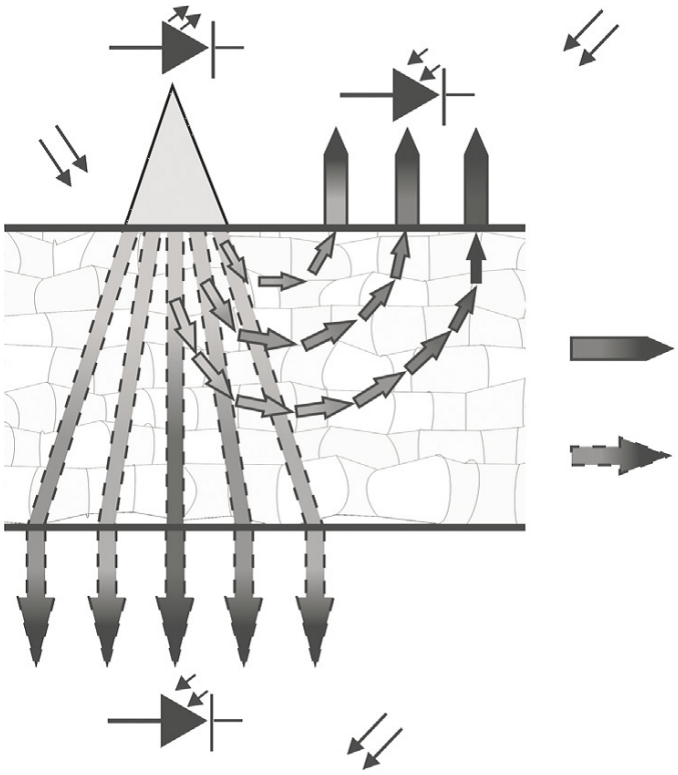

Figure 2: Transmission and reflectance mode [6].

The selection of wavelength is a compromise and relies on the targeted application, but is typically chosen between 510 to 920 nm corresponding to green and infrared lights, respectively. Measurements done on light skins and at normal ambient temperature (around 20 degree) have shown that reflected green light has an advantage regarding to the AC/DC component ratio over reflected infrared light [8]. Thus, green light is usually chosen as the light source in wristband optical heart rate monitoring (OHRM) application considering the light skin.

The depth that light can penetrates increase when the length of the wavelength increase. Thus, IR light is desirable when it needs to reach deeper tissues in below two conditions. In cold ambient conditions, the blood microcirculation decreases dramatically, then reaching deeper tissues becomes an advantage. The dark skin pigmentation, which contains high melanin concentration, absorbs wavelengths shorter than 650 nm strongly. Therefore, choice of an optimal wavelength for heart rate monitoring rely on the specific application and its usage conditions and is a balance between sensitivity during poor skin perfusion and vulnerability to artifacts.

2.2 Application

The PPG based OHRM has been applied in many different scenarios, but mainly in three areas: daily life, sports monitoring and clinical application.

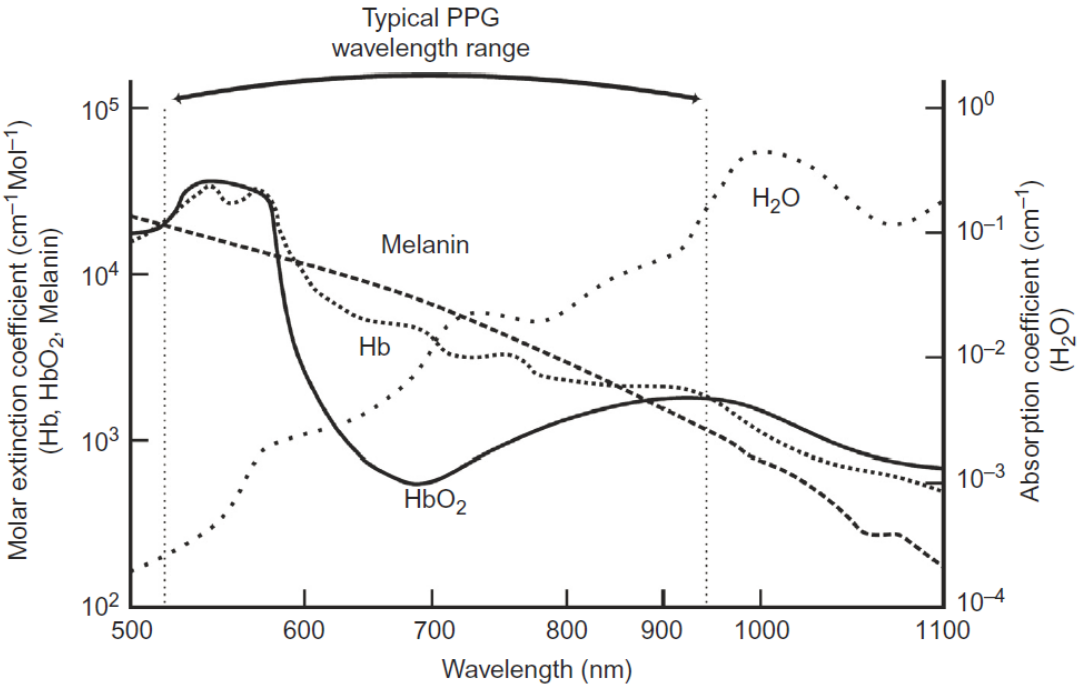

Figure 3: Absorption and molar extinction coefficients of main biological tissue constituents(H2O, Hb, HbO2, and Melanin) at 500 to 1100nm window wavelengths [6].

2.2.1 Daily life

With the development of wearable device, consumer's interest in wearable sensor beyond sports monitoring increases rapidly. HR monitoring during daily life would allow more accurate estimation of physical activity and energy expenditure [9] by combining the monitoring of acceleration which allows identifying patterns and amount of physical activity, rough sleep quality, and step count. OHRM can potentially also estimate physiological stress and recovery based on beat–to-beat HR [10].Compared to chest-strap and electrode-based solution, optical HR monitoring is more acceptable to customers for long-term use considering its better unobtrusiveness and wearability.

However, continuous heart rate monitoring in daily life is still demanding regarding the power consumption and customer requirements. A significant power consumption is inevitable in optical sensing because of constitutional power consumption of LEDs and required signal processing circuitry, and battery life should be extended to full 24 hours in a week to increase the usability. Also, a snug, comfortable and fit-to-the-skin sensor is necessary for reliable HR monitoring since poor sensor contact will increase motion artifacts dramatically.

2.2.2 Sports monitoring

HR monitoring during exercise is especially favorable in fitness workout, professional training planning or endurance training. Real-time monitoring enables users to control the training intensity to optimize training accurately by avoiding too high or too low training load. Additionally, maximal energy expenditure and oxygen uptake and can be accurately estimated from heart rate measurement. Also, use of HR monitoring will motivate users to exercise [11][12].

In 1983 the first chest-strap wearable HR monitor was produced by Polar Electro. This device consisted of two parts: a transmitter on an ECG-based chest strap and a watch receiver [13]. Currently, ECG-based chest straps are commonly used during sports to provide accurate monitoring of HR. However, chest straps have disadvantages in usability and user acceptance due to its cumbersomeness and its accuracy may be reduced with poor strap placement, dirty electrodes or dry skin.

As an alternative, optical HR monitor has been introduced to solve the user acceptance-related and usability problem in chest-strap HR monitors. Studies on the reliability of the available solutions compared to ECG-based chest strap have not been done widely. Some researches report that comparable performance can be achieved, but can be worse in a wide range of conditions, including cold conditions, vigorous movements of the body site where the sensor is placed. If changes in these conditions can be solved, optical HR monitoring during sport can replace ECG-based strap and have a wide market. According to the evaluation of accuracy and reliability of two consumer wrist-worn optical heart rate monitoring product [14], the OHRM device from PulseOn can achieve 94.5% mean reliability with an accuracy of 96.6%, compared to 86.6% and 94.3% of device from Mio LINK.

2.2.3 Clinical application

The analysis of HR variability (HRV) has been proved valid in the early detection of diabetic neuropathy and prediction of risk for acute myocardial infraction. Other promising researches have also investigated the potential of HRV in other cardiological diseases such as arrhythmias, congestive heart failure, hypertension, and sudden death or cardiac arrest [6]. In order to extract these gold-standard HRV features, the ability of detection and record of heartbeat time location is necessary for the HR monitoring device.

Clinical applications of the PPG-based HR monitoring device are at the early stage. Most of the HR-based researches can be recreated with a less inconspicuous, cumbersome and more daily-life long-term user-friendly PPG-wrist device which will not affect the behavior of the subjects. Thus, a well integrated and light PPG wristband might contribute the studies of long-term cardiovascular regulation mechanisms.

2.3 PPG signal artifact and quality

PPG signals is a result of the interactions between light propagation and tissue characteristics. As shown in Figure 4, factors affecting the PPG measurement can

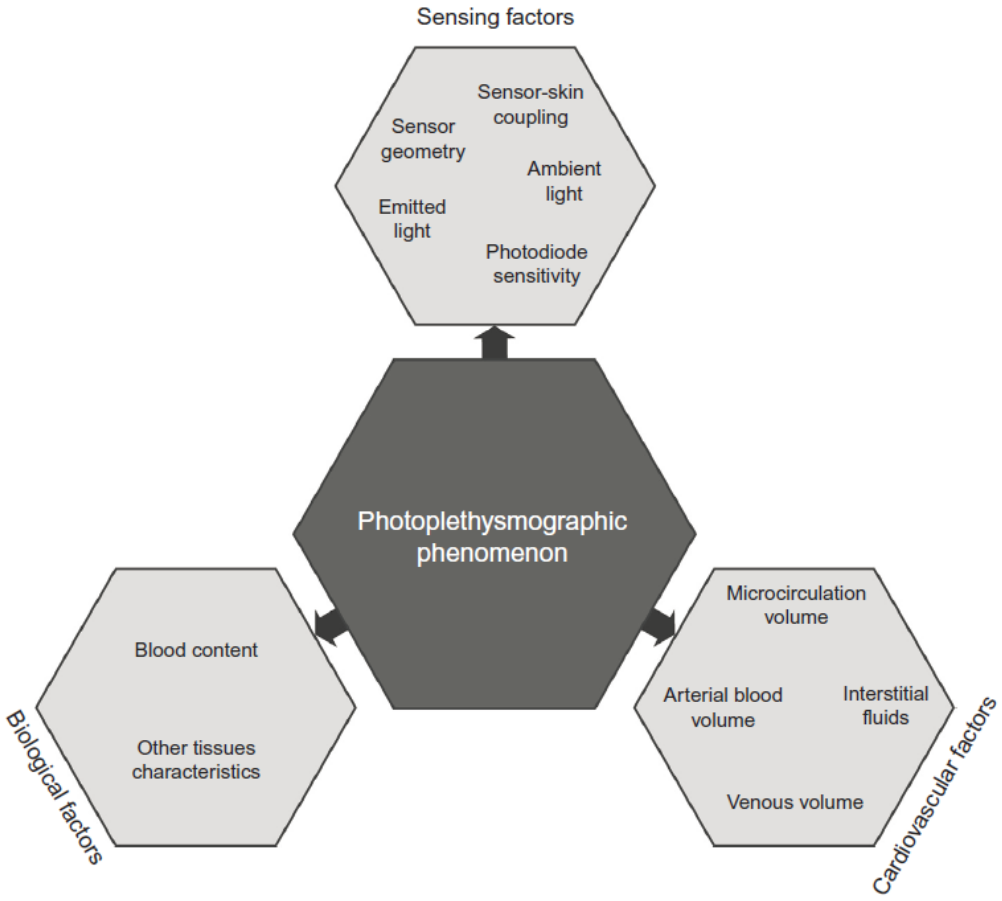

Figure 4: Three factors that affect PPG signal [6].

be separated into three categories: sensing, cardiovascular and biological factors.

The quality of PPG signal is greatly influenced by the sensing factors, including the property and amount of injected light, the coupling between the optical probe and the skin, and the response of the photodetector. The optimal distance between light emitters and receiver should be carefully chosen as a compromise between the achievable light intensity injected into the skin and the desired depths of tissue penetration. Experimental studies indicate that optimal separation distances are in the range of 6 to 10 mm [15] for infrared light and around 2 mm [16] for the green light.

Biological factors include blood content and skin pigmentation. These tissue characteristics modify the absorption and scattering properties of the tissue which will influence the amplitude of the measured PPG signal. The cardiovascular factors are related to cardiovascular stresses, age and body position and will influence the morphology and character of the PPG signals.

2.4 Motion artifact

The PPG signal is naturally sensitive to motion artifacts concerning its measurement principle. Three different artifacts have impacts on the signal quality, including tissue modifications due to movements, the relative motion of the sensor-skin interface and changes in the pressure between the optical probe and the skin. These artifacts will be illustrated below.

Voluntary movements modify the inner tissue which changes the volume of the tissues traveled by the emitted light and thus influences the signal. Voluntary movements include motion of tendons and compression or dilatation of the tissues and the muscles. Moreover, the motion-related acceleration changes the distribution of the fluid in the tissue and modify the shape of the soft tissue. These tissue modifications cause the change of the optical path and therefore modify the measured optical signals.

The optical probe is attached to the skin through some binding, which is not perfectly fixed. A global or local movement of the body part might generate a shift of the sensor relative to the skin surface. This shift modifies the optical path of injected light and thus modifies the optical signals.

The pressure generated by the probe on the skin surface modify the amplitude of the received signals. An initial increase of the pressure causes an enhancement of the pulsating component of the PPG waveforms by cause of an improvement of the optical interface between the probe and the skin. When the applied pressure exceeds some threshold value, the squashing of blood vessels will decrease the amplitude of the pulsating component [6].

To solve the influence brought by the motion-related artifacts, it is essential to model their effects on the PPG signals. A representative model of the relation between the motion and the motion artifact is obtained by combining multiplicative and additive models, possibly with nonlinear relations as shown in Figure 5. In this case, the observed signal y(t) is represented as the sum of the pulse component s(t) and a weighted multiplication of both pulse and motion components s(t) and m(t) as depicted by the following equation.

$$y(t) = (1 + \alpha...m(t)...)s(t) \tag{1}$$

The observed frequency components Y are described as the sum of pulse components S and the weighted convolution of pulse and motion components S and M as presented in the following equation.

$$Y = S + \alpha...S * M \tag{2}$$

Typically, the motion artifacts can be classified into three different categories: rhythmical motions related, intermittent and continuous non-rhythm. Generally rhythmical motions generated during endurance activities and behave as a stationary process, thus can be subtracted from the PPG signals by signal process techniques. Non-rhythmical motion artifacts are generally more challengeable to resolve. In order to estimate the HR during activity with OHRM device, a good opto-mechanical design of the probe and signal-processing algorithms are necessary.

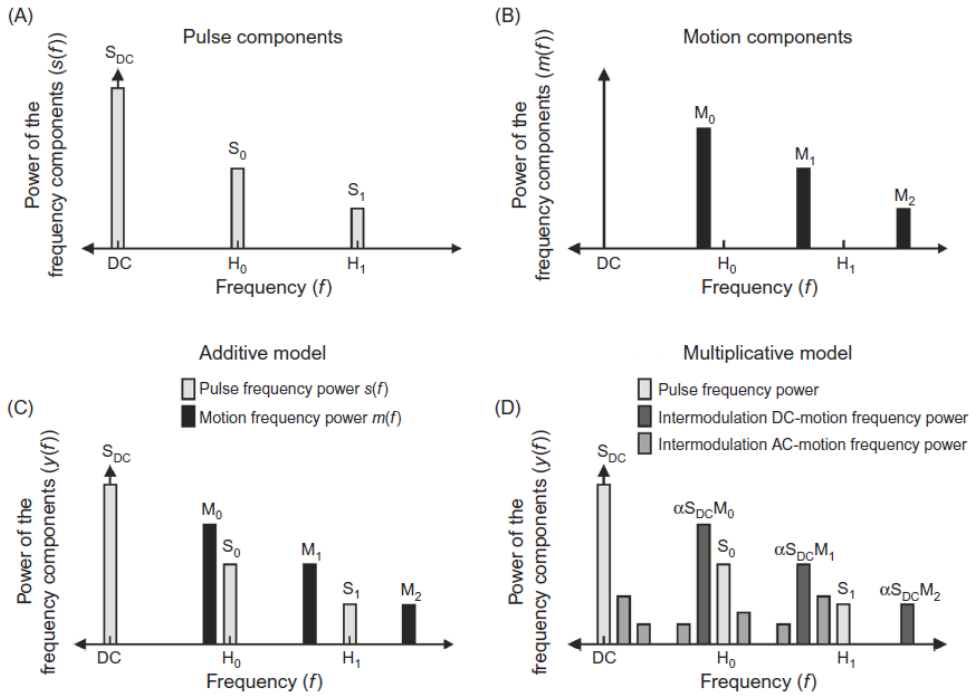

Figure 5: (a) Frequency components S of the optical pulsating signal s(t). (b) Frequency components M of the optical motion-artifact signal m(t). (c) Frequency components Y of the observed signal y(t) following an additive model. (d) Frequency components Y of the observed signal y(t) following a multiplicative model [6].

3 PPG front end

Figure 6 shows the block diagram of a typical front end. The emitted light from the LEDs passes through or reflected from the tissue and then received by the photodetector. After that, the received signal is amplified by a transimpedance amplifier. A demodulator, such as a low pass one or a high pass one, is necessary if multiple wavelengths are used to separate the signals into independent signal chains before filtered by an analog signal conditioning filter. The filtered signal is then sampled and converted to digital form through a sampled-and-hold circuit and DAC, respectively. The digital signal is sent to a microcontroller, which will perform the calculation of the physiological parameters such as heart rate and inter-beat-intervals and control the LEDs through the LED driver to get a better quality signal.

3.1 Light source

The light-emitting diode is an ideal light source for optical heart rate monitors considering its small size, large output over a narrow bandwidth and excellent drive characteristics. Besides, LEDs are compact, have a long work life, operate over a wide temperature with small shifts in the peak-emitted wavelength, and are mechanically robust and reliable. To reduce the power consumption of LEDs, LEDs are only switched on for a short interval while the photodiode is sampling the reflected light for the pulsation measurement [17].

When you turn on the LEDs, there exists a turn-on delay which is the time between the start of the electrical current pulse and the start of the optical emission. This delay is due to the initial filling of the junction capacitance of the LEDs. As shown in Figure 7, the LEDs start to emit light after the junction is charged. The charge-up time is determined by the RC time constant of the LED and the pulse current.

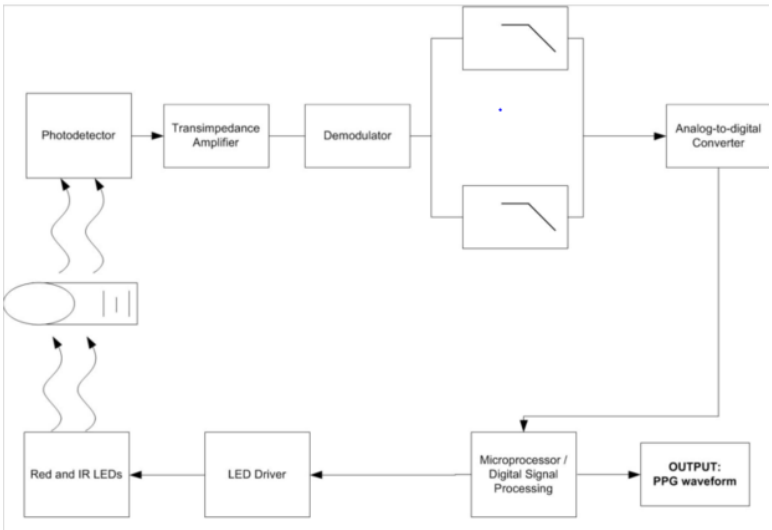

Figure 6: Block diagram of a typical PPG front end [18].

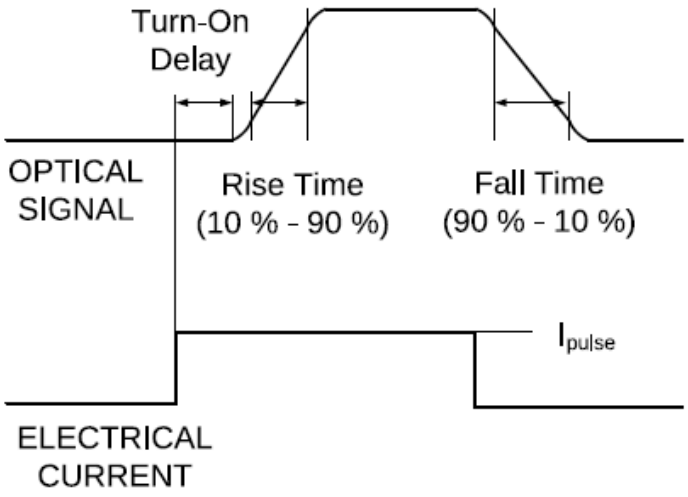

Figure 7: Typical optical response of a LED on a rectangular current pulse [19].

3.2 Typical front end

Switching time is the time it takes to switch a LED from its ON state to OFF state or vice versa. The optical rise or fall time of the LED is calculated by the equation below:

$$t_{r/f} = a_{r/f} * \frac{1}{\sqrt{k_{LED} * I_{pulse}}} \tag{3}$$

Where k_{LED} is a LED type dependent characteristic constant, $a_r = 1.49$ for the rise time and a_f =2.11 for fall time. According to this equation, the switching time of a LED depend on the pulse current; in order to reduce the switching time to half, the LED current need to be quadruped.

3.2.1 Photodetector

Photodetectors are sensors of light or other electromagnetic energy [20]. A photodetector has a p-n junction that covers light photons into the current. As an input of the OHRM device, photodetector sense the intensity of the light reflected from or transmit through the tissue and generates the corresponding current. This current is then converted to a voltage by a transimpedance amplifier.

Photodiodes are the main choice of the majority of current ORHM devices considering their size and cost, responsivity to different wavelengths, sensitivity and response time. The main characteristics that contributed their common use are list as follow [21]:

- The relatively low cost which is important for commercialization.
- Linear output current response to incident light which means no need for complicated linearization circuitry.

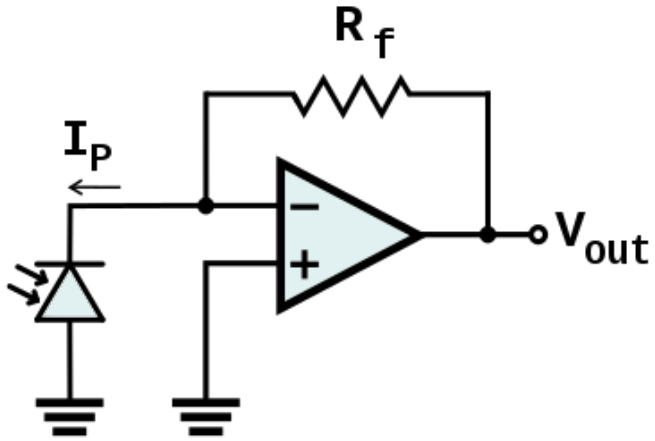

Figure 8: Simplified single-ended transimpedance amplifier[22].

- Response speed can be increased by applying a reverse bias voltage.
- Low dark current. Low current ensures that transimpedance amplifier stage after the photodiode has less chance of over-amplifying that may cause the circuit become saturated and the signal becomes useless.
- Good sensitivity which is important to achieve good signal t noise ratio for the signal, as less amplification is needed.
- Spectral response can be broad over the desired wavelengths, typical 80 – 100% relative response from 660 – 940 nm. Specially treated photodiodes can even respond with a relatively good response to lower or higher wavelength, facilitating the use of more than one wavelength of light, i.e. green or IR.
- Available in a wide variety of packaging which makes them more adaptable.

3.2.2 Transimpedance amplifier

Transimpedance amplifiers (TIA) are typically used to convert the output current of the photodiode to a voltage signal in the PPG application.

The DC and low-frequency gain of the simplified single-ended transimpedance as shown in Figure 8 is set by the equation below:

$$V_{out} = -I_p * R_f \tag{4}$$

The transimpedance gain is equal to the value of the feedback resistor. There are several different configurations of transimpedance amplifiers which suited to different applications. An advanced differential configuration is preferred in the PPG application as shown in Figure 9.

Differential transimpedance amplifier configuration can double the voltage output as given in the equation:

$$V_O = 2I_P * R_f \tag{5}$$

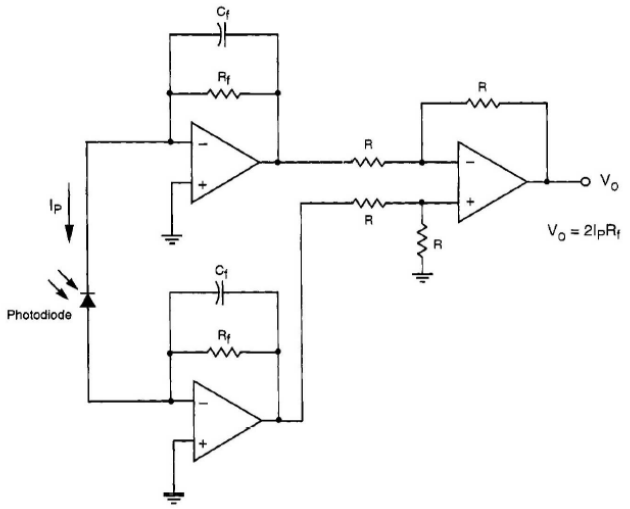

Figure 9: Differential transimpedance amplifier configuration [1].

Also, the differential configuration has the advantage to remove the common-mode rejection of coupled noise by driving the input differentially. The feedback capacitor reduce the gain peaking and improves stability. The feedback capacitor will affect the bandwidth of the TIA which can be calculated by:

$$BW = 1.4 * \sqrt{\frac{f_c}{2\pi R_f (C_I + C_f)}} \tag{6}$$

where C_f is the feedback capacitor, C_I is the total input capacitance, R_f is the feedback resistance and f_c is the unity gain frequency of the operational amplifier.

3.2.3 Demultiplexing and sampling

The output voltage of the transimpedance amplifier can be multiplexed signal which requires demultiplexing to recover the individual signal of different wavelengths. The signal obtained from the demultiplexing stage is then sampled by the sample-and-hold circuit. Figure 10 presents a sample example with LED modulation.

3.2.4 Filtering and analog-to-digital conversion

The sampled signal from the demultiplexing stage is passed through filters to remove unwanted frequencies and aliasing artifacts caused by the sample-and-hold circuit. A low-pass filter with a cut off of approximately 20 Hz is implemented to pass all PPG signal and a high-pass filter is used to remove the DC portion and extract the AC portion of the PPG signal. ADC is then implemented to digitalize the signal.

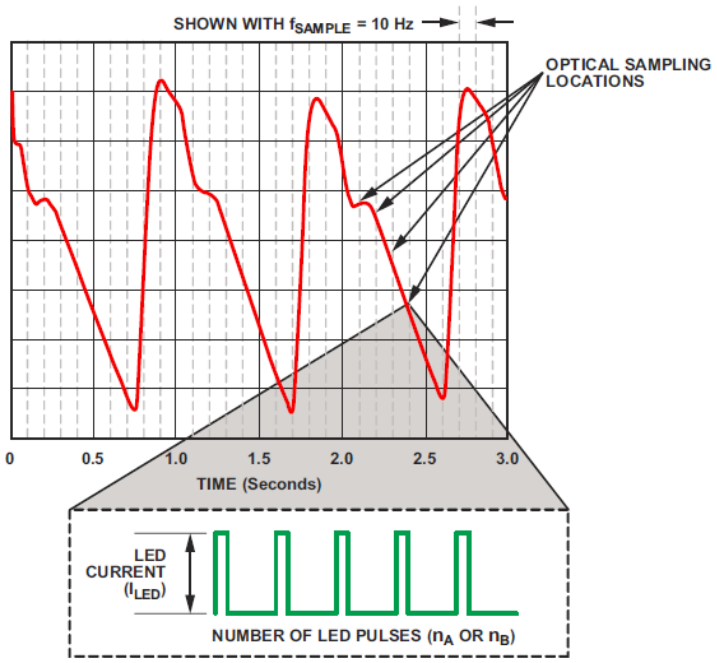

Figure 10: Example of a PPG sampling strategy where the sample rate is 10 Hz using five pulses per sample [23].

3.3 Signal process module

In every stage of the signal process chain illustrated above, the noise will inevitably be added to the measured PPG signal. Half of the total noise comes from the power supply stage due to the fact that power supply noise is directly transformed into noise in the LED driving current, which generates the noise in the LED light and received by the photodetector. Reducing the power supply noise can be achieved by professional power supply design, which suppresses the noise from the source.

The other half of the AFE noise originates mainly from the TIA and the ADC, leaving the intermediate stages for a smaller contribution [24]. TIA and ADC noise reducing can be achieved by LED modulation and dynamic range enhancement techniques.

3.3.1 LED modulation

The LEDs of OHRM device are usually time-division modulated at a high frequency to enable a single photodetector to sample more than one LEDs, reduce power consumption and noise.

The physiological signal occupies the same spectrum with static interferers and low-frequency noise, which can be removed by shifting the pulsatile signal to a field of the spectrum with less noise by modulating the LED light source. The modulated signal can then be recovered by two methods: envelope detection and product detection. An envelope detector can take a high-frequency signal as input and provides an output which is the envelop of the original. An envelope detector is

simple to implement, however, it is more susceptible to noise and may lead to signal distortion if overmodulation situation happens. The product detector multiplies the received signal by the same reference signal which is used to modulate the LEDs, then removes the noise by a filter. Even though it is more complicated to implement compared to the envelope detector, the product detector is popularly applied in PPG technology considering its ability to decode the overmodulated signal and its higher signal to noise ratio.

Square wave modulation is the most popular LED modulation scheme applied in modern AFEs. The LED driving signal are first chopped by a square wave with frequency f_s . The chopped LED light passes through the tissue and modulated by the arterial blood pulsations (which is at the heart rate f_p) amplitude. The photodiode detects the light waveform which has a small slowly-varying component at frequency f_c sitting on top of a fast square wave with frequency f_s.

The choice of the duty cycle of the LED drive pulses is a trade-off. The smaller this duty cycle is chosen, the lower its DC components will become and therefore reduce the LEDs power consumption. However, the ON duration the LEDs should be long enough to allow the photodiode to get a reliable sample. Therefore, there is also a practical power limit on duty cycle values [25].

The selection of the carrier frequency fs is also a trade-off. The lower this frequency is selected, the more rigorous the characteristic requirements (such as sharpness or roll-off) of the low-pass filters implemented in filter stage will become. On the other hand, the higher the chopping frequency is selected, the higher its duty cycle will come, which increases the power consumption.

3.3.2 Dynamic range enhancement

Considering the fact that the AC component of PPG signal could be lower than 0.1% of the total PPG signal. Therefore, if the measured signals are digitalized directly, most part of the ADC quantization range will be wasted on DC offset which contains little information. To efficiently utilize the ADC range, the DC component should be removed from the PPG signal before quantized by the ADC.

Several techniques have been implemented to enhance the PPG sensor dynamic range. Some of these techniques will be presented below.

Glaros and Drakakis [26] reported an integrated solution to remove static interferers by a digital feedback loop. The feedback loop controls the LED drive currents to subtract the reference voltage with the average output of the TIA in the second stage of the AFE. This solution requires an off-chip ADC and an external 1MHz clock and consume 800 μW.

As shown in Figure 11, a digitally assisted analog technique has been implemented to subtract ambient light from the photoreceptor [27]. The subtraction current is updated at $>$ 10 Hz intervals with properly adjusted subtraction steps. Similar digitally assisted analog dynamic range enhancer has been reported by Winokur et al. as shown in Figure 12 [28]. It includes a current digital-to-analog converter (DAC) to subtract a static amount of current from the photodiode current, an amplifier to amplify the rest of the current and a digital feedback to control both the DAC and

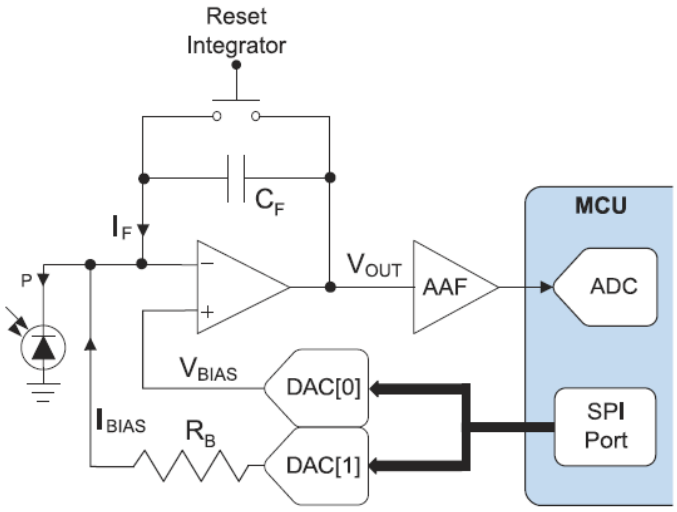

Figure 11: Diagram of the digitally assisted analog current subtraction technique by Patterson and Yang [27].

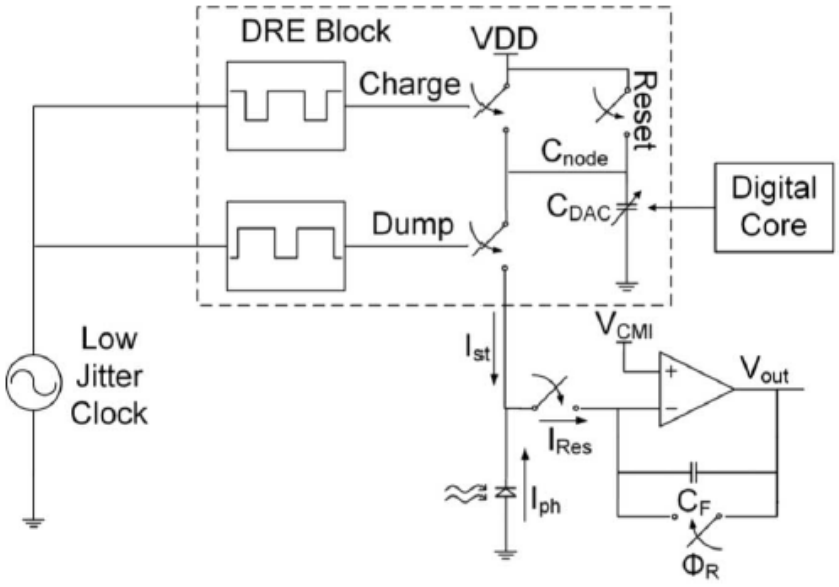

Figure 12: Diagram of the dynamic range enhancement circuit [28].

amplifier.

Both the designs of Patterson and Yang and Winokur et al. share the same idea of measuring the mean input current on the front end and directly subtracting this current from the pre-amplifier input. The saturation problem can be solved with these design and the TIA with a very high gain of the AC component can be achieved.

3.4 Parameter adjustment

The purpose of parameter adjustment is to maintain a certain parameter within the desired range including exploiting the ADC range, maintaining a minimum desired signal to noise ratio or minimize the front end power consumption. The parameter adjustment may relate to modifying the gain of amplifying stages and changing the LED driving currents or offset cancellation currents.

The monitored parameters include DC or AC value of the signal, or quality of the detected signal. Those parameters are either directly measured or calculated after processing. The control algorithms for the parameter adjustments are usually implemented with digital feedback variables generated through a DAC [29].

The control algorithms aim at keeping the input signal of the ADC proper to fully utilize the dynamic range of the ADC. Cheung et al. implemented a control algorithm with control thresholds as shown in Figure 13. If the input signal of the ADC exceeds the threshold L1 or L2, the system adjusts the LED driving currents to increase or decrease the intensity of the LED to prevent the ADC from saturation. The control threshold L1 and L2 are set slightly below the maximum of the ADC range, L3 and L4, to prevent saturation caused by rapidly shifting signals. When the input signal exceeds the desired operating range L5 or L6, the system changes the programmable subtractor to increase or decrease the subtracted offset voltage to guarantee the input signal is within the desired voltage range.

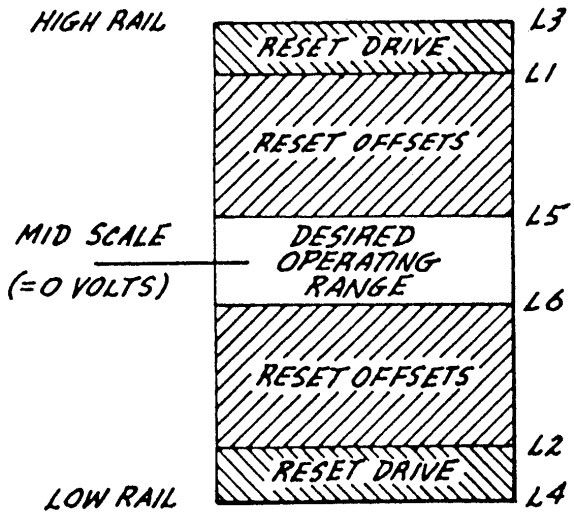

Figure 13: Threshold of the control algorithm to get desired response [30].

As presented in Figure 14, Winokur et al. implemented a complete analog front end with an integrated control system for PPG measurement. The digital feedback control both the LED driving current and dynamic range enhancement circuit. The flow diagram of the control system illustrated the work flow of the system as shown in Figure 15.

The input current I_{RES} is amplified and digitized first. If the digitized output is greater than the minimum and less than the maximum threshold, the system

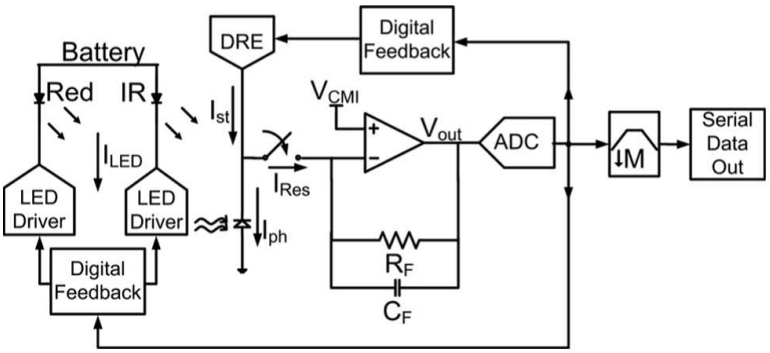

Figure 14: Block diagram of the control system designed by Winokur et al. [28].

remains unchanged and go back to the first step for next sample. Otherwise, if the output is less than the minimum threshold and I_{LED} can be increased, the algorithm increases the I_{LED} and wait for the next sample; if the I_{LED} cannot be increased, the algorithm decreases the I_{st} and reset I_{LED} to zero. The LED driving current is updated every sample, while the DRE current is updated about once per 1.5 s to ensure the stability.

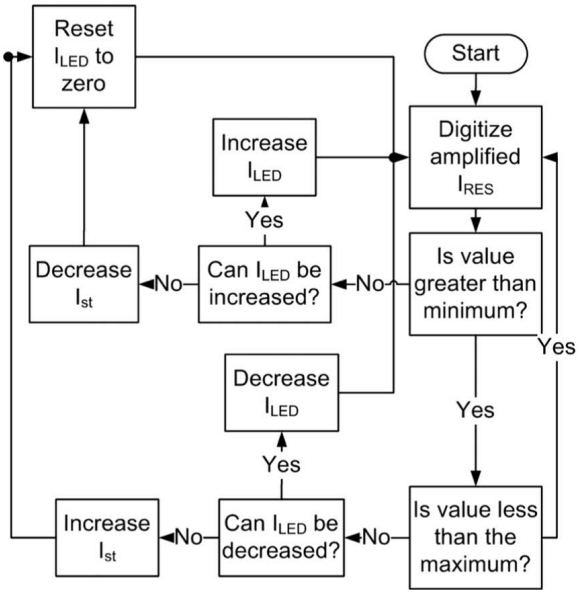

Figure 15: Flow diagram of the digital feedback algorithm in the control system implemented by Winokur et al. [28].

4 Methods

This thesis work is based on the PulseOn product development and the final channel selection implementation will be integrated into the PulseOn OHRM sensor product. After the channel selection is implemented in the PulseOn wristband with AFE4404, various tests, including accuracy and power consumption, were conducted to evaluate the performance of the device with new channel selection feature.

This section starts with the introduction of PulseOn OHRM device and AFE 4404, followed by introduction of the developing tools: Nordic nrf tools, which are used for data acquisition. Data process will then be presented to show how to deal with the raw data. The last part covers the details of the performed tests,including measurement protocol, Fitzpatrick scale for skin color and reference device.

4.1 PulseOn OHRM device

PulseOn OHRM device is a wearable wristband device that provides real time heart rate monitoring during daily life and sports. The device also provide the information of step counts and sleep quality. These user data can be synchronized to the mobile application through Bluetooth to visualize the user data.

As shown in Figure 16, the size of the device is 39.81x18.11x12.5 mm. The device has three LED indicators to indicate the current state of the device and a silicone strap for the user to wear on the wrist. There is one button in the top of the device to reset the device. On the bottom of the device are two LEDs and one photodetector to perform PPG measurements.

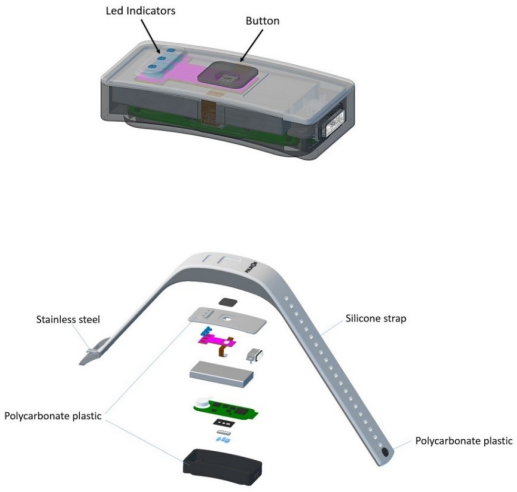

Figure 16: PulseOn optical heart rate monitoring device [31].

The device is specially designed considering the usability, comfortability and the purpose of reducing motion artifact. When the silicone strap is properly attached to the wrist, the contact between the sensor and skin will be tight enough and the

device can stay in one place to reduce possible motion artifact. Also, extra light pressure caused by the proper attachment will increase the signal quality and reduce the amount of ambient light. The sense of touch of the silicone strap is soft and comfortable and increases the friction between the the device and skin and therefore reduces the potential motion artifact.

This device consist of one green LED, one infrared LED and one photodetector. The photodetector is placed in the middle with green and infrared LEDs located on both sides of the photodetector with a distance of 2mm. All necessary components for heart rate measurement are integrated inside the device, including accelerometer, proximity sensor for off-hand detection and a MCU to perform the heart rate acquisition and data recording.

The optical sensor module of PulseOn OHRM device is BioMon Sensor SFH7060 from OSRAM. It has three green, one red, one infrared emitter and one photodetector and a light barrier to block optical crosstalk. The key characteristics of light emitter are listed in Table 1. The diagrams of relative spectral emission for green and infrared emitter are shown in Figure 17 and 18.

Table 1: Green and infrared LED characteristic of SFH7060 [32].

Color	**Green**	**Infrared**
Wavelength of peak emission (nm)	530	950
Spectral bandwidth at 50% of Imax	34	42
Rise and fall time time of Ie (10% and 90% of Ie max)	32	16

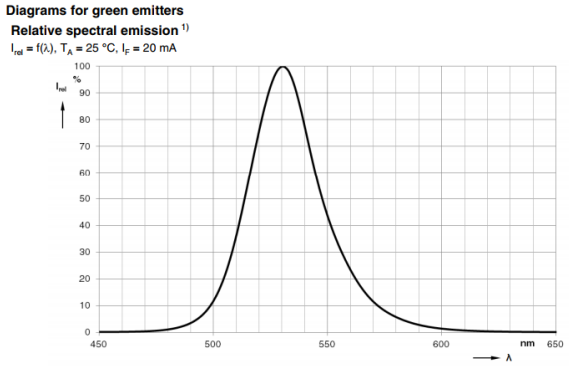

Figure 17: Diagram of relative spectral emission for green emitter [32].

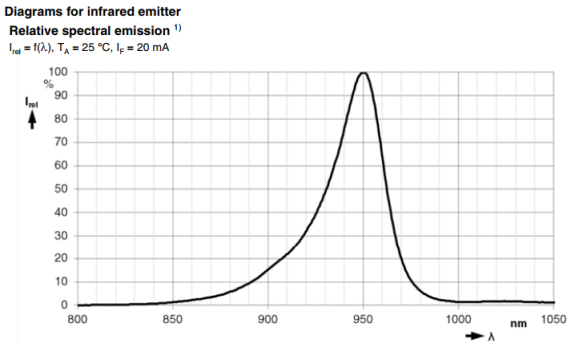

Figure 18: Diagram of relative spectral emission for infrared emitter [32].

The photodetector of module SFH7060 has a spectral range of sensitivity from 400 to 1100 nm and the rise and fall time is 2.3μs (V_R=3.3V,R_L=50Ω,λ=940nm). The relative spectral sensitivity for the detector is shown in Figure 19.

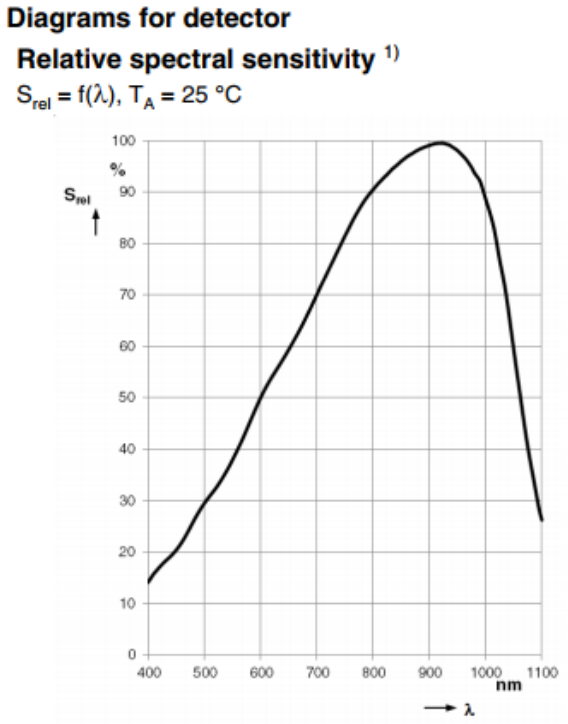

Figure 19: Diagram of relative spectral sensitivity for photodetector of SFH7060[32].

4.2 AFE4404

The AFE4404 is an analog front-end manufactured by Texas Instruments for optical bio-sensing application, such as heart rate monitoring, pulse oximetry and heart-rate variability monitoring. The device consists of three switching light-emitting diodes and one single photodiode. The current signal generated by the photodiode is converted into a voltage signal by the transimpedance amplifier (TIA) and digitized

by an ADC. The ADC output can be read out using an I2C interface. The AFE also has a fully-integrated LED driver with a 6-bit current control. A high dynamic range transmit and receive circuitry is applied to sense very small signal [32].

The simplified block diagram of the AFE4404 is presented in Figure 20. The AFE has an integrated transmitter and receiver for optical heart-rate monitoring and pulse oximetry applications. The pulse repetition frequency (PRF) determines the repetition periodicity of a sequence of operations of the system. Each cycle of a PRF generates four 24-bit digital samples at the output of the AFE, each of which is stored in a separate register [32].

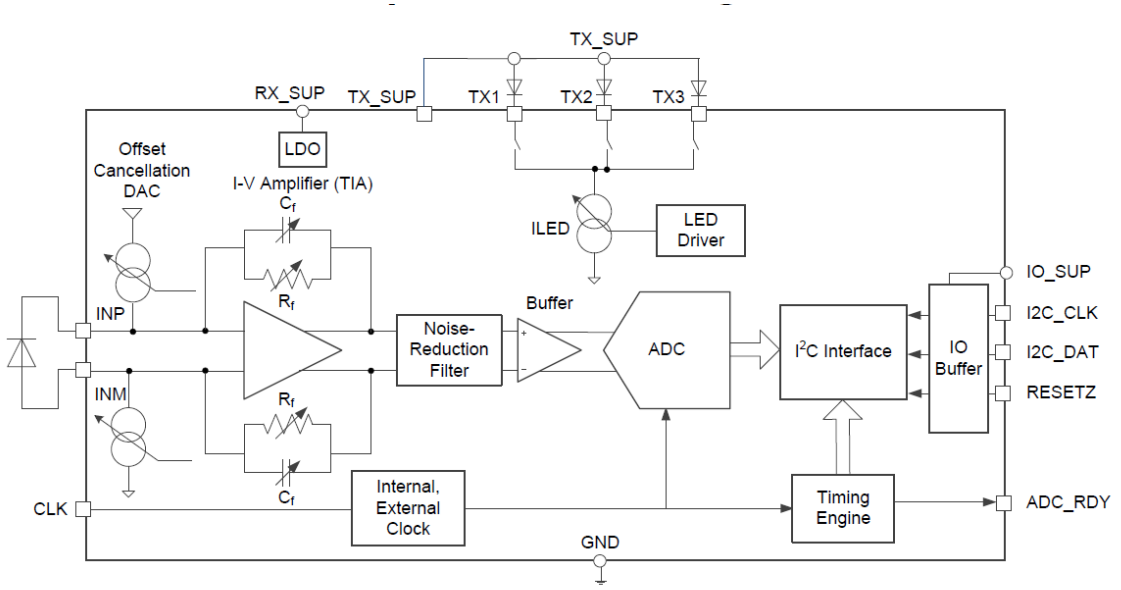

Figure 20: Simplified block diagram of the AFE4404[32].

The LED driver can control the LED current intensity from 0 mA to 40 mA through a 6-bit LED current control. The received current signal from the photodiode is converted to a differential voltage by a TIA. The TIA gain is determined by it feedback resistor(R_f) and can be programmed from 10 $K\Omega$ to 2 $M\Omega$. The transimpedance gain between the input current and output differential voltage of the TIA is 2xR_f . The bandwidth of the TIA is restricted by the C_f and R_f. And the product of C_f and R_f gives the time constant of the TIA and must be set as approximately 1/5 or less of the LED durations. The Noise Reduction Filter consists of four parallel instances of the switched RC filter, each of which are connected to the TIA output during one of four sampling phases. The output of the Noise Reduction Filter is then converted into a digital signal with an ADC. The digitalized signal can be read out through the I2C interface.

One of the significant improvement of AFE4404 is the offset cancellation DAC at the input of the TIA. As discussed in the previous section, a PPG signal has a DC component and an AC component. To efficiently utilize the dynamic range of the TIA, a programmable cancellation current is set based on the DC current signal

level to remove the unwanted DC component and amplify the AC component which contains the PPG information.

The ADC provides a 22-bit representation of the current from the photodiode. The ADC codes corresponding to the various sampling phases can be read out from the 24-bit register in two's complement format. The two MSBs of the 24-bit word work as sign-extension bits to the 22-bit ADC code as shown in Table 2. These sign-extension bits are imported while dealing with overflow situation.

Table 2: Green and infrared LED characteristic of SFH7060

Differential input voltage at ADC input	**24-bit ADC output code**
-1.2 V	1110 0000 0000 0000 0000 0000
(-1.2/2^(21)) V	1111 1111 1111 1111 1111 1111
0	0000 0000 0000 0000 0000 0000
(-1.2/2^(21)) V	0000 0000 0000 0000 0000 0001
1.2 V	0001 1111 1111 1111 1111 1111

The AFE4404 also implements a dynamic power-down feature to reduce power consumption, which is used to shut down the receiver inside every cycle. This dynamic power-down feature can be configured by setting the start and end point of the power-down phase in the time engine.

4.3 Data acquisition

This part presents the tools used for data communication between the PulseOn device and the computer.

The nRF52 development kits are used as the bridge between the wristband device and computer. Furthermore, the nRF52 Command Line Tools are used for development, programming, and debugging of the device. The command line tools for Linux operation system are selected as the development environment is in a Ubuntu12.04 operation system. The used commands for erasing, programming and reset the device are shown in Table 3.

Table 3: Commands and corresponding description of related command lines.

Commands	**Description**
nrfjprog –family NRF52 –eraseall	Erases all user available program flash memory and the UICR page.
nrfjprog –family NRF52 –program	Programs the specified HEX file into the device. If the target area to program is not erased, the –program operation will fail, unless an erase option is given.
nrfjprog -f nrf52 –program,–sectorerase	If –sectorerase is given, only the targeted non-volatile memory pages, excluding UICR, is erased.
nrfjprog -f nrf52 -r	Performs a soft reset by setting the SysResetReq bit of the AIRCR register of the core. The core will run after the operation.

After compiling and generating the target HEX file from the makefile, the HEX file can be programed into the device by the nrfjprog command line tool. Before the programming, it is necessary to first erase the program flash memory, otherwise, it will fail. To update the specific application without erasing the whole program flash memory, the command –sectorerase can be added to erase the targeted non-volatile memory pages. As for resetting the program, command –r can be used.

The nRF connect for Mobile is a powerful generic tool that allows users to scan, advertise and explore Bluetooth low energy (BLE) devices and communicate with them. In this thesis work, the nRF connect application is used to send commands to the device for controlling purpose, including switching between different work mode, configuring data output format, recording data, and performing flash memory operations.

After connecting to the device, select Unknown Service from the operation page. Then press the upload button next to Unknown characteristic and select TEXT from the drop-down menu to send the commands. The commands and corresponding actions are shown in Table 4. In practice, the default settings for entering sampled mode and printing out all raw data can be set in the codes and only commands related to recording, dumping and erasing data is needed during data collections.

Table 4: Commands and corresponding action for nRF Connect Mobile application.

Commands	**Action**
S	Entering continuous mode which measures HR continuously.
L	Entering sampled mode which measures HR periodically.
2	Print out data: ACC and PPG.
4	Print out data: TIA settings change.
5	Print out data: algorithm results (HR & steps)
r	Start recording to flash.
R	Stop the the recording to the flash.
d	Dump Flash drive through cable.
e	Empty flash from previous recordings.

The data are first transferred from the flash memory of the wristband to the nrf52 development kit and then sent to the computer. As shown in Figure 21, the communication between the flash and nrf52 is carried out by the Serial Peripheral Interface bus (SPI), which is a synchronous serial communication interface specification used for short distance communication, primarily in embedded systems. The UART is chosen to send data from the nrf52 to the computer.On the computer side, a text-based modem control and terminal emulation program, minicom, is selected to receive and save the data into TXT file in the terminal. The receive file will then be processed by the Matlab script to visualize the PPG signal and to calculate the performance.

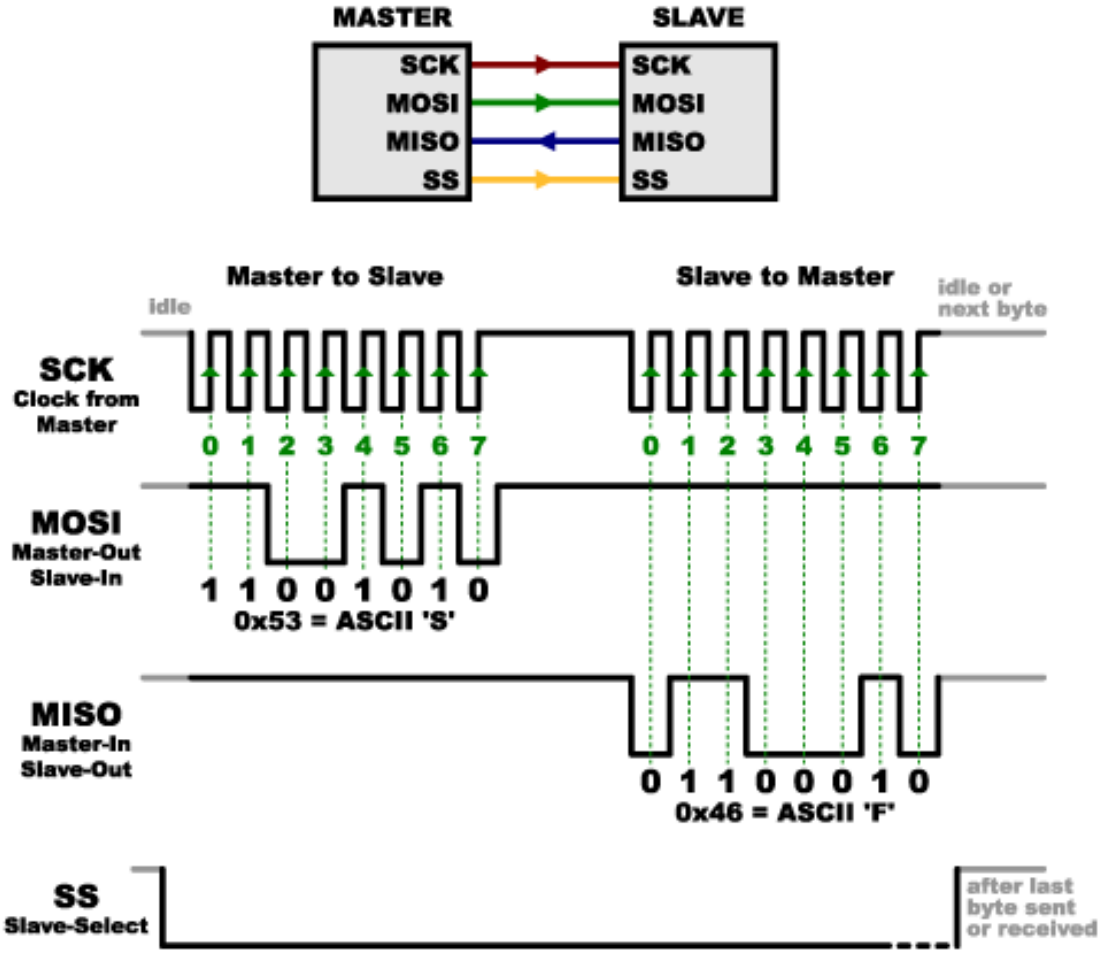

Figure 21: SPI communication between the nrf52 development kits and the wristband [33].

4.4 Processing of raw data

For the purpose of Matlab simulation, the raw data file needs to be processed and generate a Matlab data file with the extension .MAT, which is the input of the channel selection algorithm. While for data collected from the device which

implement the channel selection algorithm, the behaviors of the channel selection, heart rate reliability and error matrix will be plotted.

4.5 Performed tests

This section introduces the Fitzpatrick scale for classifying the skin color types, treadmill, reference device and measurement protocol for evaluating the performance of channel selection, as well as the anthropometric parameters of the measured subjects.

4.5.1 Fitzpatrick scale

In order to investigate the effect of skin color on the performance of each channel and the channel selection algorithm, a classification of skin color is necessary. In this thesis, Fitzpatrick scale is applied to classify the skin color types. The Fitzpatrick scale is a numerical classification scheme for determining the skin color based on a questionnaire related to an individual's genetic constitution, reaction to sun exposure, and tanning habits. The response to each question is added up to get a final score corresponding to the Fitzpatrick skin type as shown in Figure 22. Fitzpatrick scale is widely accepted to assess the skin type [34].

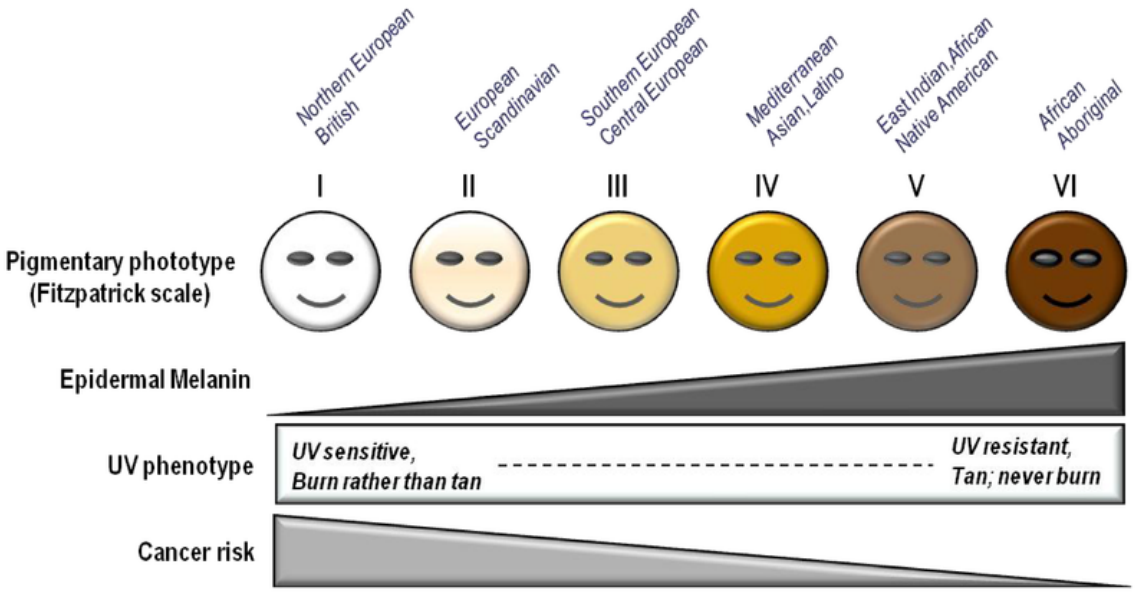

Figure 22: Fitzpatrick scale used for skin color classification [34].

4.5.2 Treadmill

A treadmill is used to perform the walking and running tasks as shown in Figure 23. The speed of the treadmill can be adjusted through the button on the operation panel and the time of the exercise length is shown in a small screen on the top. And this machine is capable of covering the top speed in the measurement protocol.

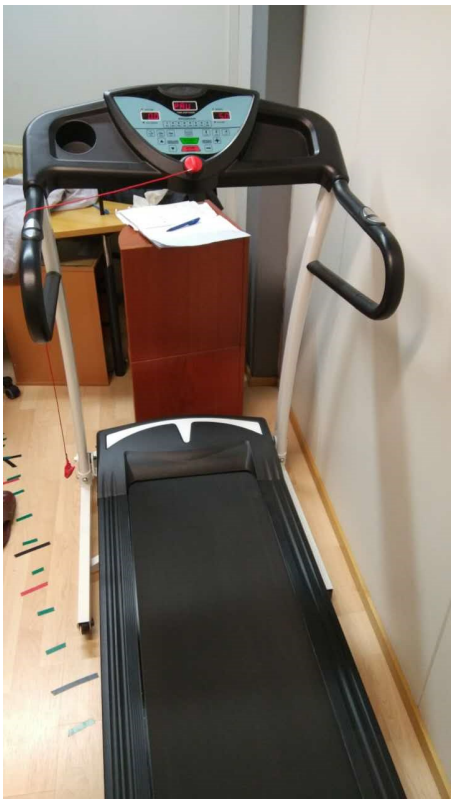

Figure 23: Running machine for walking and running tasks; photo shot by the author.

4.5.3 Reference device

The reference device, Garmin soft strap premium heart rate monitor, is used to validate the data collected from the PulseOn OHRM device. Garmin monitor will wirelessly transmits heart rate to the compatible device for instant feedback. The strap is made of soft fabric and is adjustable according to the size of user. The validation work is done in the data collection stage of Matlab simulation. As shown in Figure 24, the reference device is worn directly on the skin, below your sternum and should be snug enough to stay in place during measurement. The reference signal is used to validate accuracy of the heart rate obtained from PulseOn OHRM device.

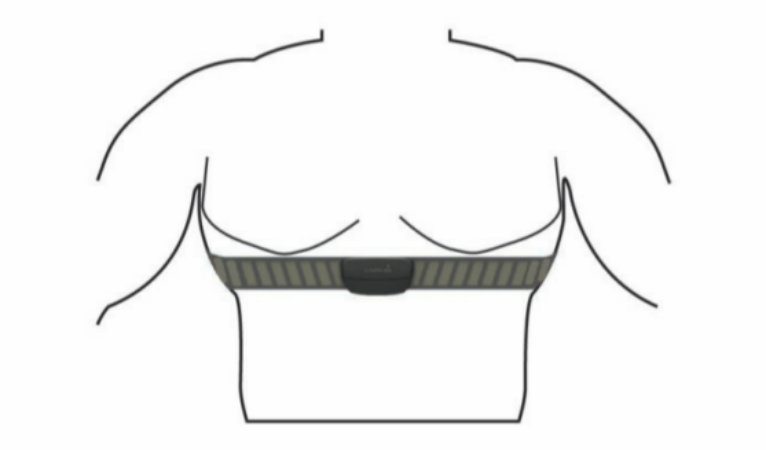

Figure 24: Garmin reference device attached to the body [35].

4.5.4 Measurement protocol

To evaluate the performance of the channel selection implementation, a properly designed measurement protocol is necessary. Below are several factors that need to be considered while designing this protocol.

- The length of sample interval
- The change between two activities
- Various activity types
- Different level of tightness

To collect more samples from the measurement, the length of the sample interval is set to the minimum which is one minute. And the duration of each activity has to be at least twice of the sample interval to get the representative data of current activity. To investigate the influence of switch of activity type on channel selection algorithm, a rest task is introduced between walking or running at speed 5, 7 and 9 km/h. After running at 9km/h task, a running at 11/12 km/h task is performed to test how motion artifact affects the decision of the channel selection. A two minutes slow walking is given to help the tester to recover from the intensive running. As shown in Table 6, the measurement will be repeated with three different tightness level to investigate the impact of the tightness.

The data collections are performed on three subjects with different skin colors. The details of the measured subjects are listed in Table 5. Subject D and E is the source of the data sets used in Matlab simulation. While the data collections for evaluation of channel selection is performed on three subjects with skin color scaled from 2 to 6.

Table 6: Measurement protocol for channel selection algorithm.

Task	Duration(Min)	Start time	End time
Rest	02:00	00:00	02:00
Walking(5km/h)	03:00	02:00	05:00
Rest	02:00	05:00	07:00
Walking(7km/h)	03:00	07:00	10:00
Rest	02:00	10:00	12:00
Running(9km/h)	03:00	12:00	15:00
Rest	02:00	15:00	17:00
Running(11/12km/h)	03:00	17:00	20:00
Walking(5km/h)	04:00	20:00	24:00

Table 5: Anthropometric parameters of the measured subjects.

Subject	**Age**	**Gender**	**Weight (Kg)**	**Height**	**Wrist size(cm)**	**Skin color**
A	25	Male	80	176	15.5	4
B	32	Male	84	174	16.5	2
C	29	Male	83	180	16.5	6
D	30	Male	73.8	178.5	16	2
E	28	Male	86.7	190	17	2

5 Channel selection

PulseOn's optical heart rate monitoring device is working in continuous mode to collect PPG signal every second, which consume a large amount of power when green channel is used. To reach a longer running time with limited battery, IR light can be applied to measure the PPG signals considering the fact that power consumption of IR LED is 27% of that of green LED. Besides, IR light has an advantage in reaching deeper tissue. Thus, IR is desired in cold condition or with dark skins.

The green light is usually chosen as the light source in wristband optical heart rate monitoring application considering its advantages in terms of AC/DC component ratio over reflected IR light on the light skin and normal ambient temperature. However, IR light can have better performance compared to green light when measurement with dark skin or in cold ambient temperature. Therefore, a channel selection between green and IR channel can combine both advantages of green and IR light by selecting the right channel in a specific scenarios. With channel selection implemented on the device, the power consumption of the OHRM device can be reduced by switching to IR channel if reliable heart rate can be obtained through IR channel. In addition, more reliable heart rate can be detected by switching the specific light channel on if this channel can have better performance regarding various measurement scenarios.

This section starts with a general introduction of work modes of the device, followed by the description of the channel selection in the Matlab simulation and implementation on the device. The author scripted an auto-test process to optimize the Matlab simulation process for the purpose of evaluating the power consumption and accuracy of channel selection algorithm with different parameters. After that, the author implemented the channel selection algorithm on PulseOn's OHRM device, followed by the evaluation of the performance of channel selection algorithm on different skin colors and tightness levels.

5.1 Work modes

Continuous heart rate measurement is required only during active exercise. During daily life, a regular interval of the heart rate measurement is implemented for reducing the power consumption. In some situation, heart rate measurement is requested on demand, for example, when the user request for current heart rate. To address different requirements, several operation modes are implemented as shown in Table 7 in an order of increasing power consumption. For example, the heart rate measurement is performed every second in sports mode to get the data continuously, while in sampled mode, the device start measurements every sample interval.

Table 7: PulseOn OHRM device operation modes.

Mode	**Description**	**Typical use case**
Idle	Sensors off, minimal power consumption	Device not worn
On demand	Activity tracking, HR on demand after a delay	Low activity
Sleep	Special mode for sleep analysis	Sleep analysis
Sampled	Activity tracking, periodic HR measurement	Normal daily activity
Sports	Continuous activity tracking and HR	Sports activity

In this thesis work, sampled mode is selected during performing channel selection algorithm. In the sampled mode, the activity, sleep, heart rate, and heart rate variation algorithm are enabled, the optical heart rate sensor is running periodically.

5.2 Matlab simulation

5.2.1 Channel selection simulation

Matlab is a high-level language and interactive environment to design the systems. The matrix-based MATLAB language is a nature way to express computational mathematics and the built-in graphic make it easy to visualize and get insights from data.

This thesis work uses MATLAB to simulate sampled mode of the device from data collected from the continuous mode and perform the channel selection process with the sampled mode.

The raw data collected from the flash of OHRM wristband is a mix of three different types of data sets with message IDs (4,5,6). The data output format is either .csv or .txt file with columns separated by a semicolon. The important items in the raw data is described in Table 8.

Table 8: Description of important items in collected raw data.

Data	**Description**
Acceleration X, Y, Z	Acceleration signal of X,Y,Z dimensions of wristdevice.
Green LED PPG	The PPG signal measured from green channel.
Green LED ambient	The detected ambient light during the measurement of green PPG data.
IR LED PPG	The PPG signal measured from IR channel.
IR LED ambient	The detected ambient light during the measurement of IR PPG data.
TIA gain-green/IR	The TIA gain value of green or IR channel.
LED current-green/IR	The LED current of green or IR LED.
HR	The measured heart rate in this sample.
HR quality	The reliability of this measured heart rate.

A data process script is written to separate three different types of data into three .txt files and generate a .mat file which contains all the information in the

raw data. The .mat works as the input of the channel selection script. The channel selection script can be divided into 6 sections. Initial setup section includes adding the internal PulseOn toolbox for heart rate estimation and setting the expected sampling frequency. The next section selects the .mat file as an input of the channel selection algorithm, followed by process of continuous mode heart rate estimation for both the green and IR channel. In section 4, a data structure containing the sampled heart rate is created from continuous heart rate estimation, then the channel selection algorithm is implemented to combine the green and IR channel into one selection result structure. The result of the channel selection algorithm is then visualized in the final section. One example figure of the channel selection result is shown in Figure 25.

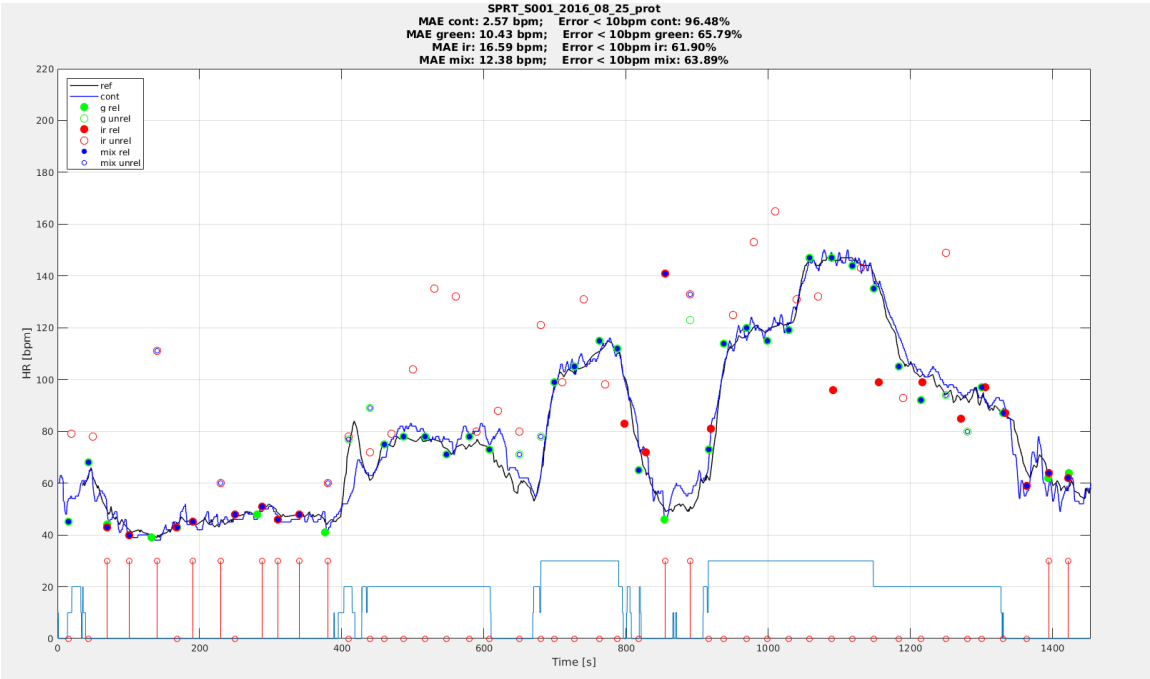

Figure 25: Example figure of the channel selection simulation by the author.

The continuous heart rate of green and IR channel is plotted in the continuous line with different color. While the estimated heart rate from the sample period of green and IR channel is plotted in circles with red and green color, respectively. The hollow circle means than the estimated heart rate is unreliable, while the reliable heart rate is represented in a filled circle. The selected channels are marked with small blue filled circles.

5.2.2 Channel selection algorithm

The block diagram of channel selection algorithm is shown in Figure 26. There are two assumptions behind the selection algorithm based on the literature researches. The first assumption is that the PPG signal obtained from the green channel is better than that from IR channel which means reliable heart rate is more likely to be

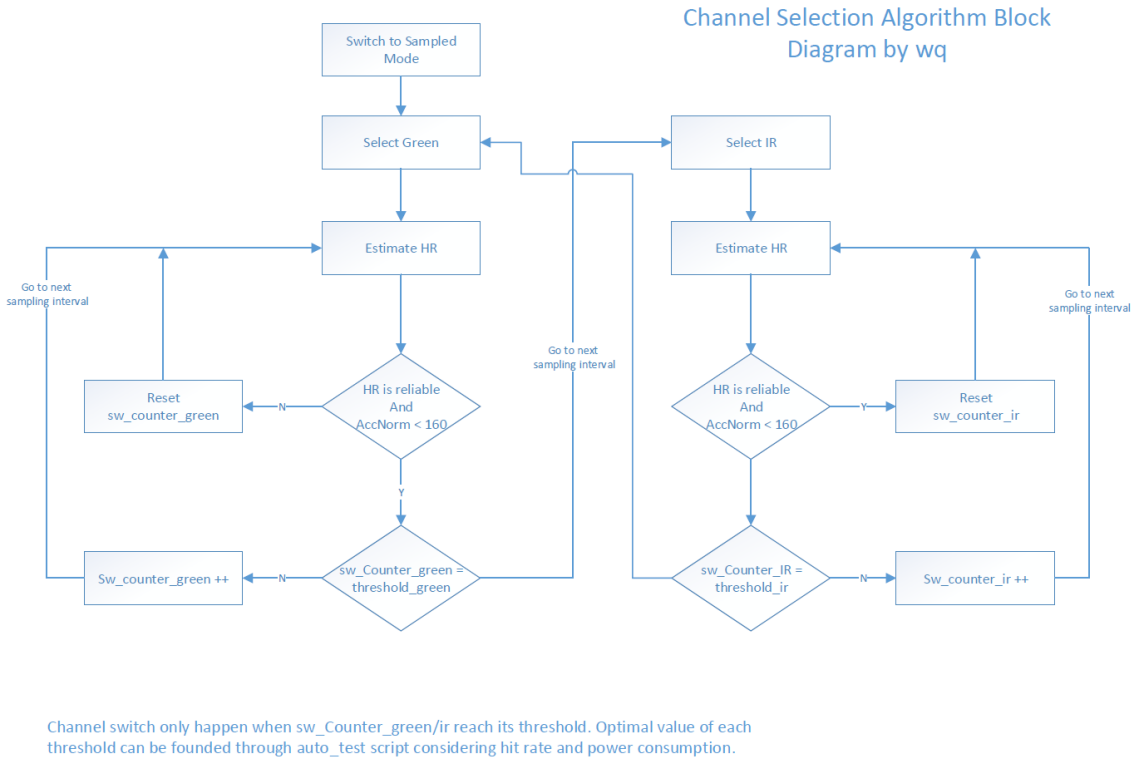

Figure 26: Block diagram of the channel selection algorithm designed by the author.

measured through green channel. The second one is related to motion artifact. The effect of motion artifact increase with the increase of the acceleration of the device, which will distort the PPG signal. The PPG signals generated from infrared light are more sensitive to the motion artifact compared to green light. Therefore, the algorithm will try to switch to the infrared channel to reduce power consumption if a reliable heart rate can also be measured from the infrared channel. Otherwise, the algorithm will switch back to the green channel to get a reliable heart rate.

First, the working mode of the device is switched from continuous mode to sampled mode. The algorithm starts from selecting the green channel and estimating the heart rate during the sample period. If the estimated heart rate is reliable and normalized acceleration is less than normalized acceleration threshold acc_norm, the algorithm then checks the $sw\_counter\_green$. If the $sw\_counter\_green$ is equal to $threshold\_green$, the channel is switched to IR channel in the next sampling interval; otherwise, the algorithm increases the value of $sw\_counter\_green$ by one and go the next sampling interval without changing the channel. If the estimated heart rate is not reliable or the normalized acceleration is larger than acc_norm, the $sw\_counter\_green$ will be reset to zero and go to the next sampling interval for next heart rate estimation.The value of normalized acceleration threshold, acc_norm, is empirically setup according to the observation of the measurement. A similar process is applied after switching to IR channel except that the judging condition of quality

of estimated heart rate and normalized acceleration is inversed. That means the algorithm will try to switch back to the green channel if the estimated heart rate is not reliable or normalized acceleration is larger than empirically.

5.2.3 Parameter tuning and corresponding power consumption

The purpose of setting *sw_counter_green* parameter is to guarantee that the algorithm switches to IR channel when the reliable heart rate can be collected in a certain long period whose length is determined by the value of *threshold_green*. This is to prevent the unnecessary switching to IR channel when a reliable heart rate is measured and normalized acceleration is less than acceleration threshold in one unstable sample period.

As for the value of normalized acceleration threshold, it comes from the evaluation of the performance of both green and IR channel in measurement protocol 1. In practice, this value works fine.

The power consumption of green and infrared LED and AFE is shown in Table 9. The power consumption is calculated by the formula below:

$$Powerconsumption = (Peak\_current * Duty\_cycle) * Voltage \quad (7)$$

Table 9: Power consumption of LEDs and AFE [32].

	Peak current (mA)	**Duty cycle**	**Average current (mA)**	**Voltage (V)**	**Power (mW)**
Green LED	50	2.56%	1280	3.6	4.608
IR LED	10	3.46%	346	3.6	1.2456
AFE TX_SUP	0.005	100%	0.005	3.6	0.018
AFE RX_SUP	0.2	100%	0.2	3.6	0.72
AFE IO_SUP	0.02	100%	0.02	1.8	0.774
AFE + Green LED	-	-	-	-	5.382
AFE + IR LED	-	-	-	-	2.0196

The power consumption of green LED is 4.6mW, which is 3.7 times of that of IR LED. And the total power consumption of AFE and LEDs of green channel is 2.66 times of IR channel, which means the power consumption of the device can be reduced to more than half if the chance of selecting the IR and green channel is the same.

An *auto_test* script is written to evaluate the performance of channel selection algorithm with different settings(threshold value of green and IR) on all the input data set in the *auto_test* folder. The output is figure that shows the performance(reliable rate and power consumption) comparison of different settings.

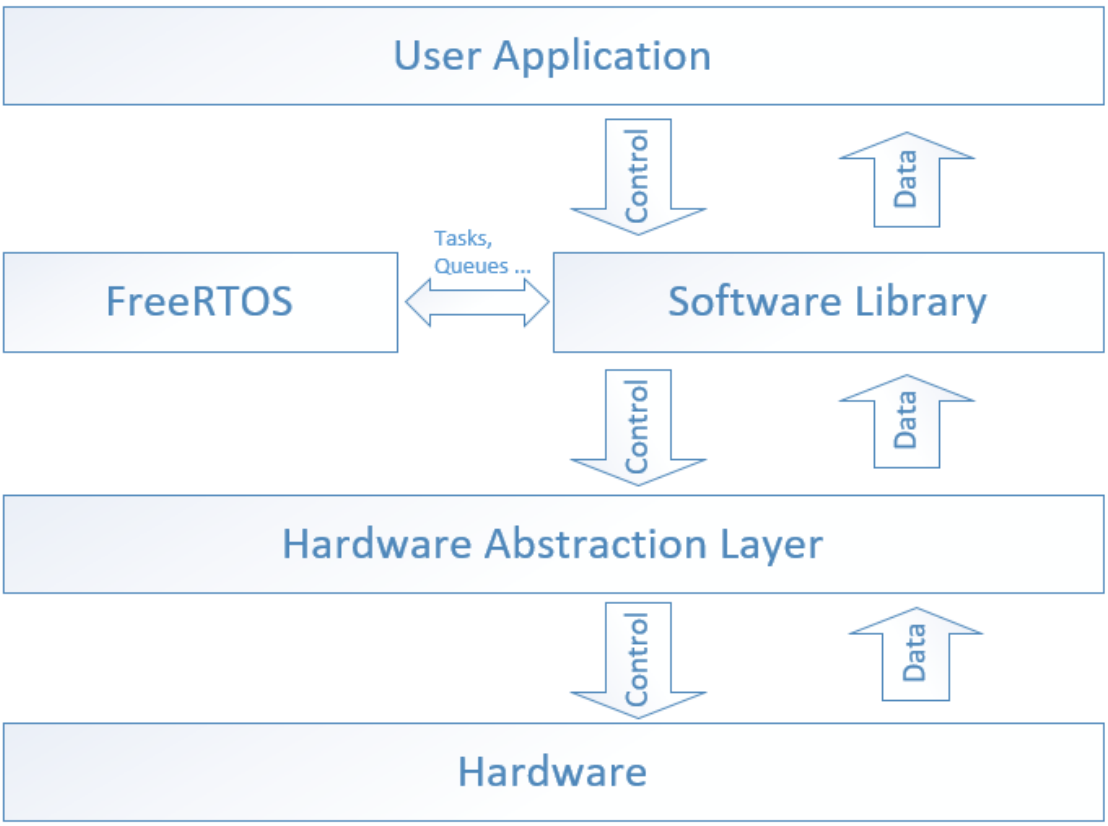

Figure 27: General software architecture of PulseOn.

5.3 Implementation on the device

This section illustrate the general software architecture of the PulseOn library, which is the base of this thesis work.

5.3.1 General software architecture

The general software architecture of PulseOn is shown in Figure 27. The software library is built on the Hardware Abstraction Layer (HAL) on the bottom along with FreeRTOS tasks, queues, mutexes and semaphores on the left. The software library also provides an API for the user to customize their user applications.

The HAL provides the library with access to the sensors and power management functions and it depends on only the FreeRTOS queues. The PulseOn library will instantiate numerous FreeRTOS tasks, for running long-term computations and performing time-critical actions, e.g., reading data from sensors.

6 Results and analysis

This section presents the results of Matlab simulation and measurements from PulseOn OHRM device with different skin colors and different tightness level. The effect of switching threshold of each channel on the power consumption and reliable rate is given and influences of the skin colors and tightness levels on the performance of the channel selection algorithm are presented in this section, as well as the improvement of the channel selection algorithm.

6.1 Simulation result of Matlab script

The auto-test script performs channel selection algorithm on three data sets in the chosen folder with different sets of threshold values of green and ir channel. Two of the simulation data sets are collected from skin type 2 in Fitzpatrick scale and the other one is from type 4. And a sports protocol is used for the data collection in the simulation as shown in the appendix. The average power consumption and reliable rate of each channel of different settings are given in Figure 28.

As discussed in the previous section, the value of switching threshold of each channel influence the frequency of channel selection. The algorithm will repeat the validation of heart rate quality and normalized acceleration until the counter reaches the switching threshold of the channel before switching to another channel.

The reliable rate of the channel is defined as the ratio of the number of reliable heart rate obtained from this channel and the total number of this used channel. Reliable rate indicates the accuracy of the selected channel.

The formula of average power consumption of each channel is given below:

$$Average\_power\_consumption = (number\_selected\_green\_channel * 5.382mW + number\_selected\_ir\_channel * 2.0196mW)/number\_total\_channel \quad (8)$$

As shown in Figure 31, among the test data sets, a minimum average power consumption is achieved when the value of switching threshold of green and IR channel is 0 and 2, respectively. This means IR channel is preferred when lower power consumption is required. The algorithm should switch to IR channel once the condition is satisfied and only switch back to green channel when two successive unreliable heart rate is detected or two successive normalized acceleration is larger than 160.

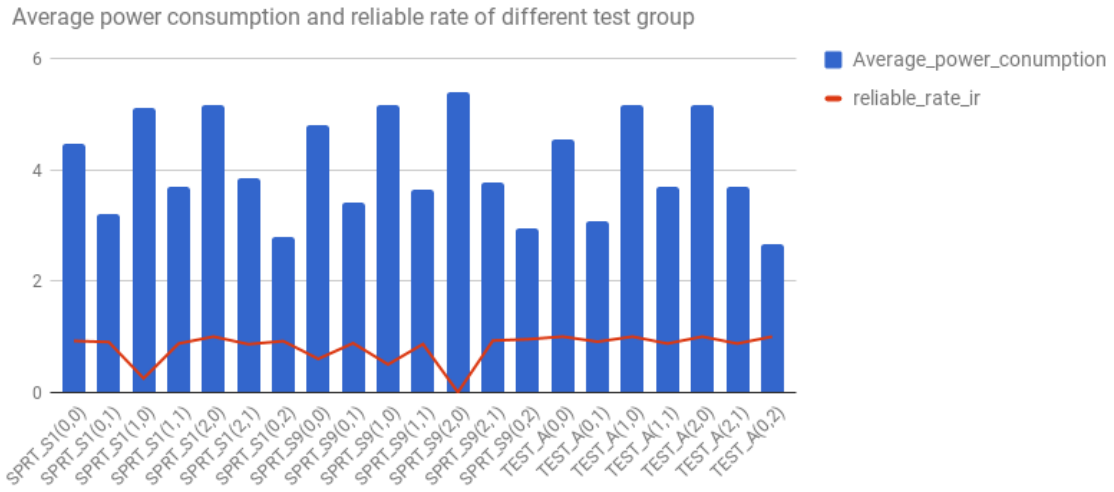

Figure 28: Total power consumption and reliable rate of each channel of different settings.

After simulating the channel selection algorithm, the total power consumption is reduced by 28.46%. And the number of selected green and IR channel are 396 and 254, respectively.

6.2 Tightness level and selection choice

An initial increase of the pressure causes an enhancement of the pulsating component of the PPG waveforms by cause of an improvement of the optical interface between the probe and the skin. When the applied pressure exceeds some threshold value, the squashing of blood vessels will decrease the amplitude of the pulsating component [36]. Therefore, the tightness level of the wristband device will affect the quality of the PPG signal and therefore influence the channel selection.

Three different levels of tightness are tested on three different skin color to investigate the impact of the tightness on the channel selection. As an example, the behavior of the channel selection algorithm with different level of tightness on the dark skin is shown in Figure 29, 30 and 31 .

When the wristband is loosely attached, the ambient light received by the photodetector is larger than those of two other levels of tightness and is much easier to be affected by the motion movement. Therefore, there are more unreliable heart rate measurements in the condition of loose attachment. For dark and light skin color, while the wristband is tightly attached to the wrist, there are much less unreliable heart rate measurements compared to the condition of the loose attachment. And the infrared channel is selected among almost all the samples.

In conclusion, the user should wear the OHRM device with a proper attachment to reduce motion artifacts and obtain reliable heart rate measurements.

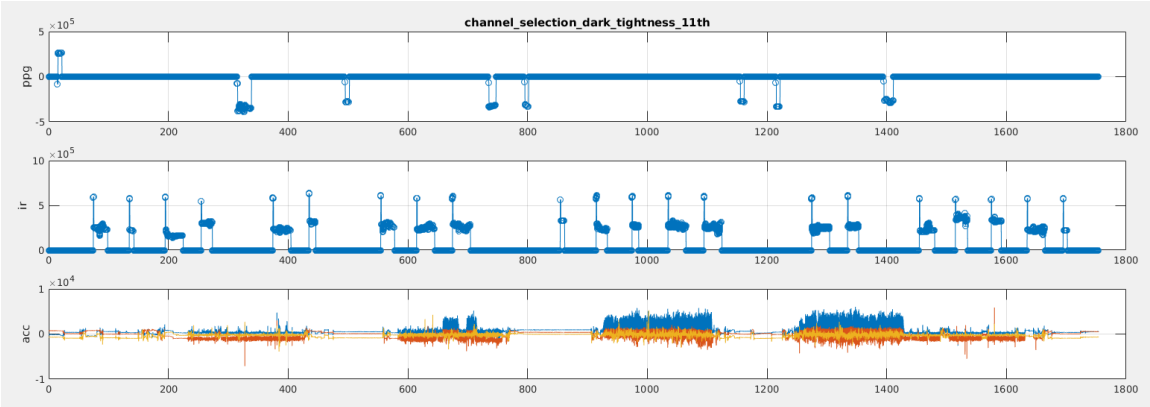

Figure 29: Behavior of the channel selection algorithm with Loose attachment on dark skin.

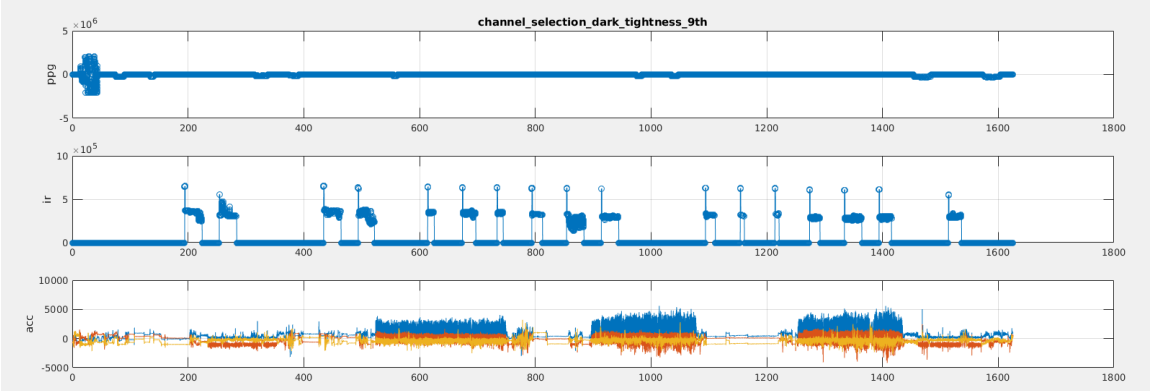

Figure 30: Behavior of the channel selection algorithm with proper attachment on dark skin.

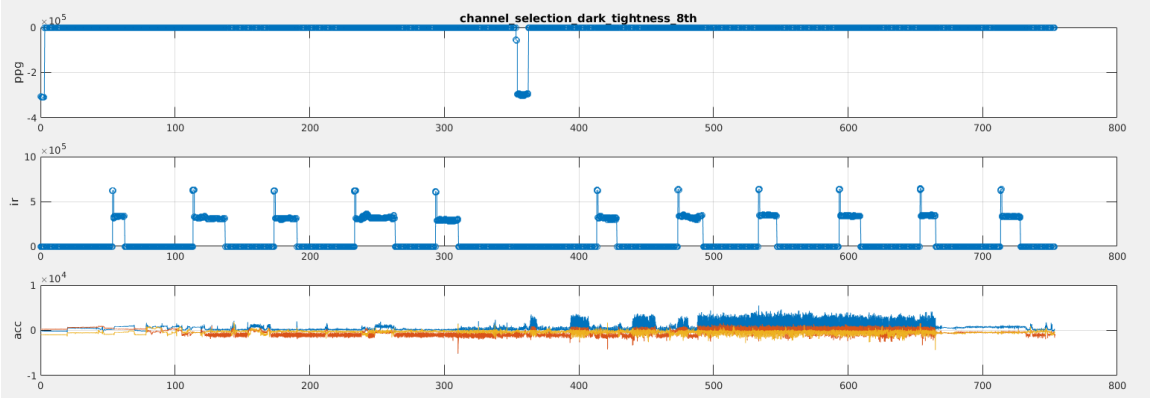

Figure 31: Behavior of the channel selection algorithm with tight attachment on dark skin.

6.3 Effect of skin color

The analysis of the impact of skin color on the channel selection algorithm is based on the data collected from proper attachment. According to Fitzpatrick scale, the white, light and dark skin colors in this thesis paper are corresponding to scale 2,4 and 6. Note that the analysis will focus on the data collected from walking and running activities. The behaviors of the channel selection algorithm with proper tightness with different skin colors are shown in Figure 32, 34 and 36. The acceleration information and heart rate reliability is also included in figures mentioned above.

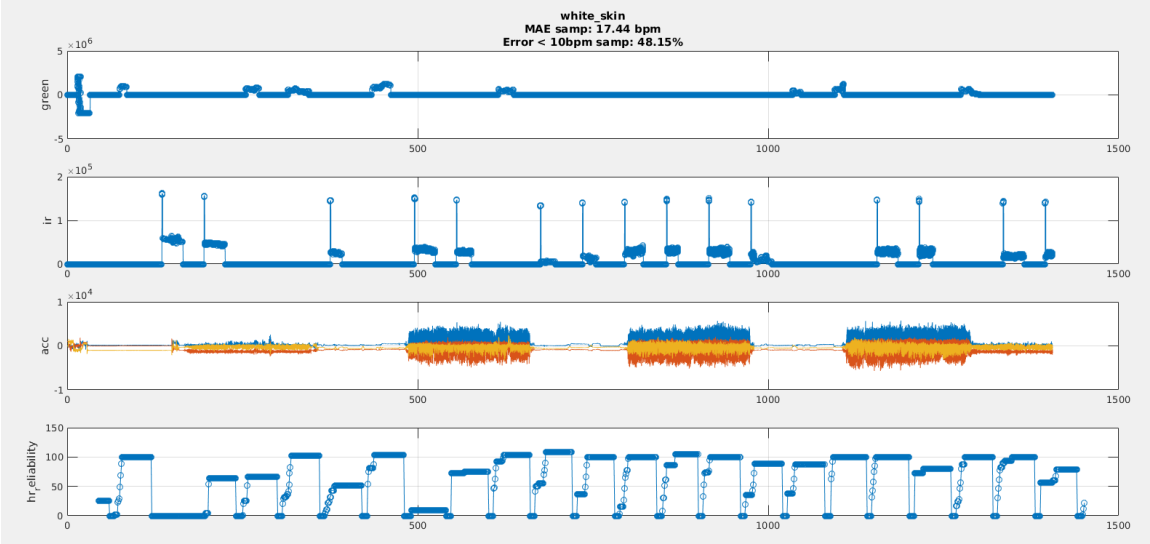

Figure 32: Behavior of the channel selection algorithm with proper attachment on white skin.

Quality index of each heart rate measurement is used to estimate the quality of heart rate measurement of different skin colors with green and IR channel. As shown in Table 10, the average heart rate quality of green channel decreases as the scale of skin color increases, while the average HR quality of IR channel increases. This means the priority of light channel is related to scale of skin color. For example, the green channel is more reliable than IR channel when scale of skin color is small then or equal to 2, while the IR channel is more reliable and should be pre-dominantly selected when scale is larger than or equal to 4.

The heart rate measurements from PulseOn OHRM device and Gramin reference device on white, light and dark skin are shown in Figure 33, 35 and 37. The changes of heart rate measurements from PulseOn OHRM device and Garmin reference device match the patter of the used measurement protocol as shown in Table 6. However, these two measurements are not perfectly matched, which could causes a bigger mean absolute error. The mean absolute error (MAE) of these three tests is 17.46 bpm, 16.46 bpm and 29.41 bpm, respectively. While the MAE of the channel selection simulation on continuous data collection is 12.38 bpm as shown in Figure 25. And the reliability(% of samples with error $<$ 10bpm) of PulseOn OHRM device with native channel selection algorithm is 48.15%, 38.46% and 17.24% for white, light and

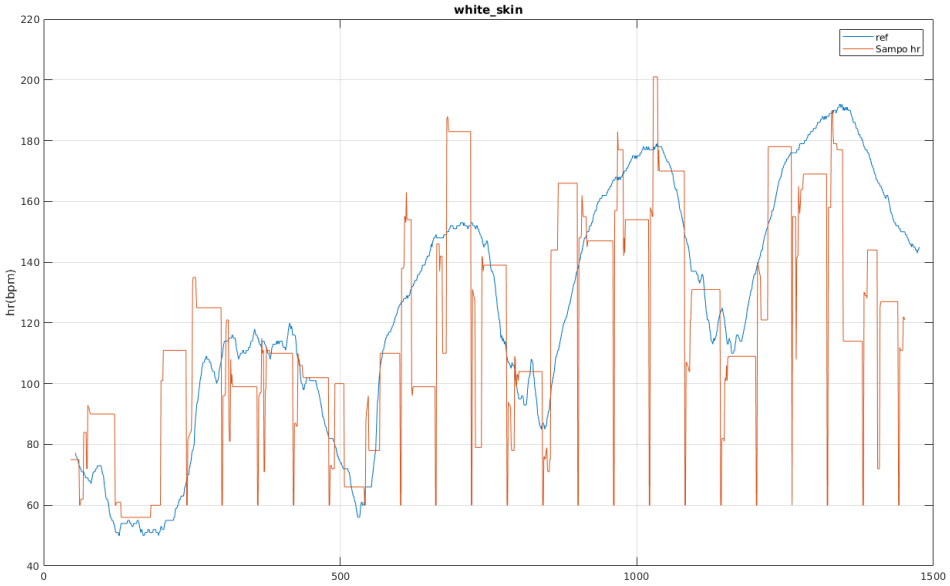

Figure 33: Heart rate measurements on white skin from PulseOn OHRM device and Garmin reference device.

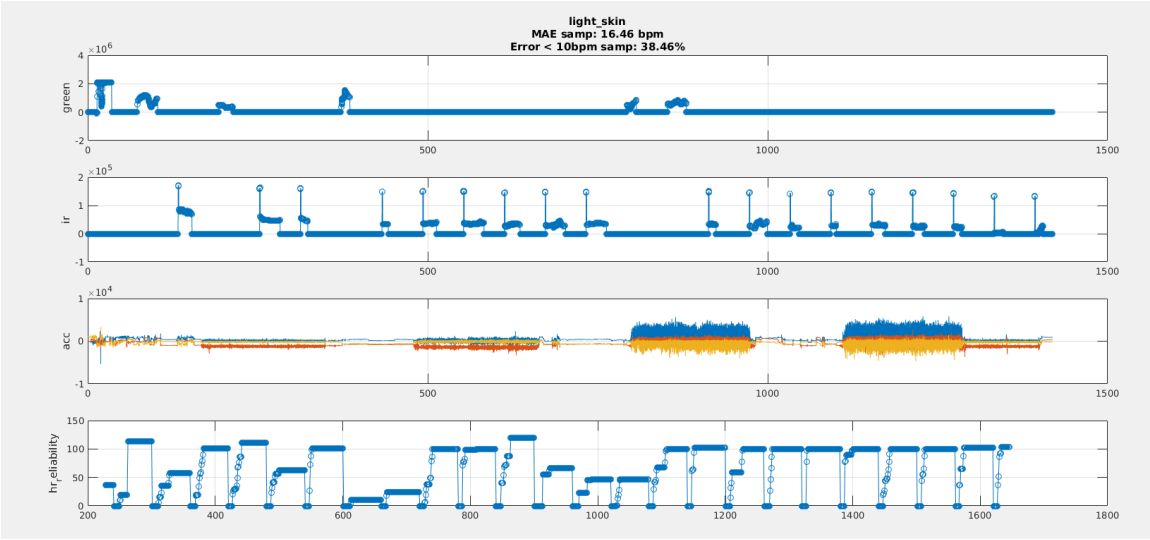

Figure 34: Behavior of the channel selection algorithm with proper attachment on light skin.

dark skin color.

As shown in Figure 32, 34, 36, reliable heart rate can be detected from IR channel on all tested skin scale even though the tester is running at 11km/h, which means the algorithm should not switch back to the green channel if the detected heart rate is reliable. In the switching algorithm, the channel will be switched back to the green channel if the heart rate is unreliable or the normalized acceleration is larger than

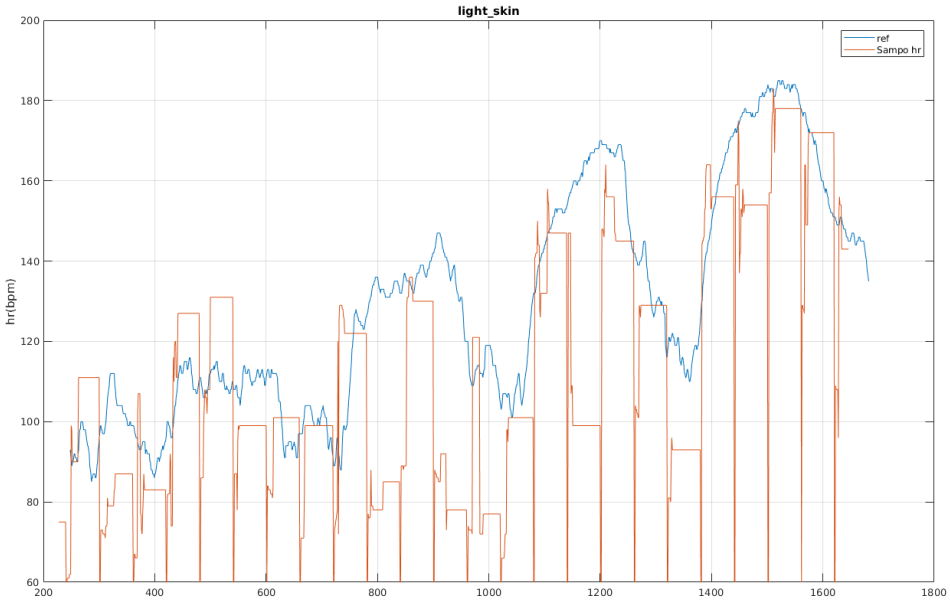

Figure 35: Heart rate measurements on light skin from PulseOn OHRM device and Garmin reference device.

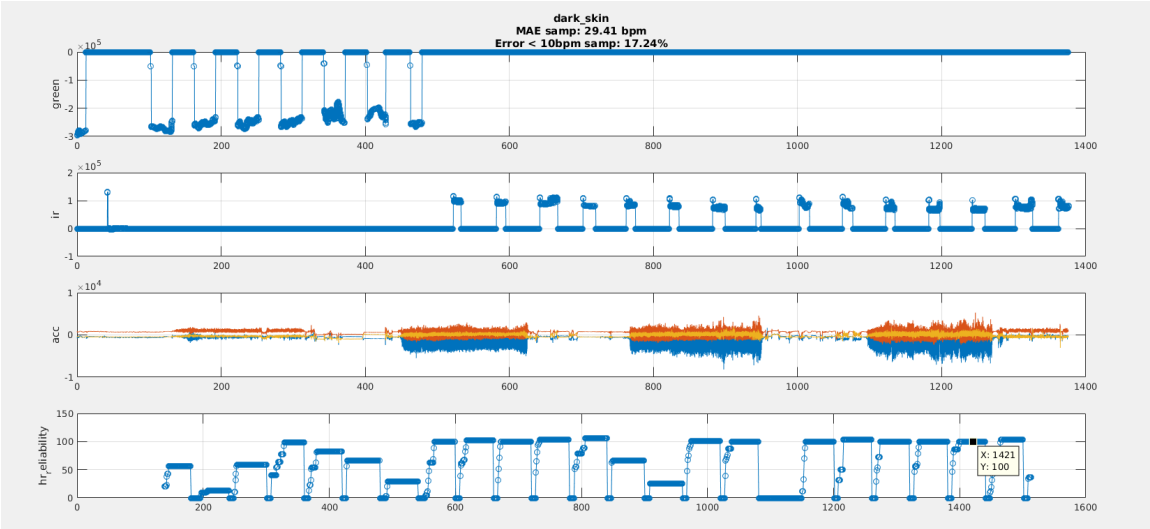

Figure 36: Behavior of the channel selection algorithm with proper attachment on dark skin.

160. This condition that green channel is more reliable is suitable when the scale of skin color is small. It can be solved either by changing the switching policy to switching back to green channel only if the detected heart rate is unreliable or by raising the threshold of the normalized acceleration.

The equation 7 is used to calculate the average power consumption of the device with different skin color and the performance of the channel selection algorithm is

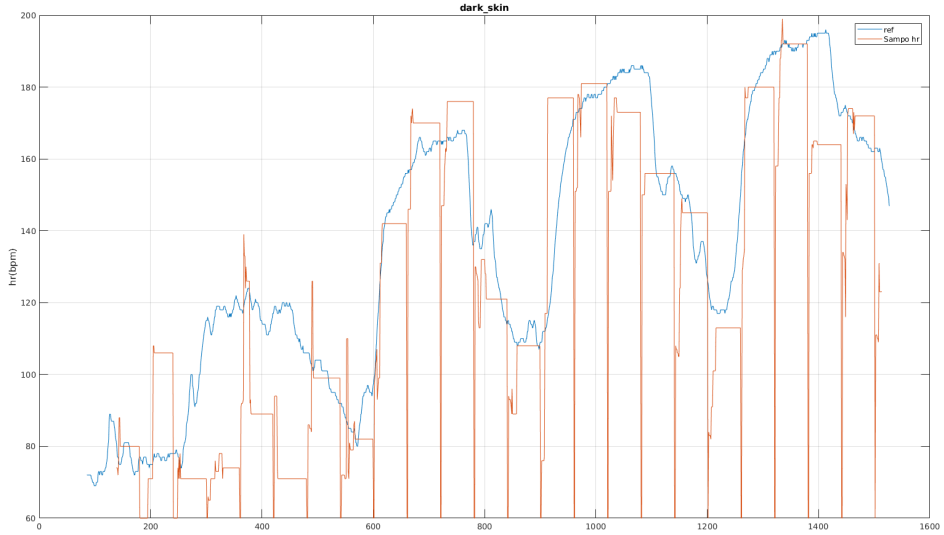

Figure 37: Heart rate measurements on dark skin from PulseOn OHRM device and Garmin reference device.

Table 10: Average heart rate quality of green and IR channel on white, light, and dark skin

Average HR quality	Green channel	IR channel
White skin	90.02	77.0
Light skin	74.33	92
Dark skin	64.14	91.2

shown in Table 11.

6.4 Algorithm improvement

The design of channel switching condition are based on two assumptions:

1. Quality of PPG signal obtained from green channel is better than that from IR channel.

2. Green channel should be selected if the acceleration is over certain threshold.

Table 11: Average power consumption of wristband with different skin color.

Skin color	**Average power consumption (mW)**	**Power consumption reduction rate (%)**
White	3.23	39.98
Light	3.23	39.98
Dark	3.096	42.48

Assumption 1 does not hold when scale of skin color is larger than or equal to 4. As for assumption 2, the value of the normalized acceleration threshold is set to 160 during the experiments for all skin color. However, according to the collected data, the value of the normalized acceleration threshold is related to the skin color, which means different threshold value should be applied for different skin color in order to achieve a better and more reasonable channel selection.

Considering the fact that the simulation data is collected from white and light skin color, the algorithm can be improved by switching back to green channel only if the obtained heart rate is unreliable. The new channel switching condition is applied in the Matlab simulation and the comparison is given in Table 12.

After the improvement, the power consumption reduction rate increases from 28.46% to 47.57% and the number of times of the IR channels are used increases from 254 to 425 without decreasing the reliable rate. The reliable rate of IR channel increases from 88.98% to 92%. The performance of IR channel is now much better than expected and can be selected in most situation to reduce the power consumption.

When scale of the skin color is larger than or equal to 4, the reliability of IR channel is higher than green channel. Thus, only IR channel should be used in this case considering the heart rate reliability and power consumption.

Table 12: Comparison of the Matlab simulation result after the algorithm improvement.

	Before improvement	**After improvement**
Power consumption reduction rate	28.46%	47.57%
Total green channel used (reliable rate)	396 (100%)	226 (100%)
Total IR channel used (reliable rate)	254 (88.98%)	425 (92%)

7 Conclusion and future improvement

The channel selection algorithm can fully utilize the advantages of each channel by switching to proper channel according to current status. The utilization of IR channel can not only reduce the power consumption but also help to handle the measurement on dark skin or cold ambient temperature. Although, the research by Fallow, Bennett A etc.[37] indicates that green light is better than IR during rest and exercise across all skin types in terms of signal-to-noise ratios. The IR light can outperform green light considering power consumption and heart rate reliability as mentioned below.

After implementing the channel selection algorithm on the PulseOn OHRM device, around 40% reduction of average power consumption is observed among all the measurements. From the view of obtaining reliable heart rate, the IR channel should be selected for the purpose of power saving when the acceleration of the wrist is less than a certain threshold in the activities, for example, when the running speed is less than 10km/h.

The behavior of channel selection algorithm is affected by several factors: including the skin color, tightness of the attachment and activity types. A fixed switching rule cannot handle measurements on all skin colors. Therefore, the skin color should be taken as the input of the channel selection algorithm and specific switching rules corresponding to different skin color are necessary to make the channel selection algorithm more adaptable.

Considering the effect of the tightness, a proper tightness would be suggested to obtained reliable heart rate estimation for white skin regardless of the activity types. And for light and dark skin, a tight attachment of the device is preferred if the activity level is higher than the equivalent intensity of running at 11kmh, otherwise, a proper attachment is good enough to acquire reliable heart rates.

In the future, more data collections of different skin colors need to be collected to develop and improve the channel selection rules for different skin colors. The optimization of channel selection is an iteration between the algorithm developments and data collections, thus, machine learning mechanism can be introduced to find the optimal normalized acceleration threshold and the switching counter threshold for each channel for different skin colors and activity types.

References

[1] J. G. Webster, *Design of pulse oximeters*. CRC Press, 1997.

[2] J. A. Patterson, D. C. McIlwraith, and G.-Z. Yang, "A flexible, low noise reflective ppg sensor platform for ear-worn heart rate monitoring," in *Wearable and Implantable Body Sensor Networks, 2009. BSN 2009. Sixth International Workshop on*. IEEE, 2009, pp. 286–291.

[3] B. Lee, J. Han, H. J. Baek, J. H. Shin, K. S. Park, and W. J. Yi, "Improved elimination of motion artifacts from a photoplethysmographic signal using a kalman smoother with simultaneous accelerometry," *Physiological measurement*, vol. 31, no. 12, p. 1585, 2010.

[4] Y.-s. Yan, C. C. Poon, and Y.-t. Zhang, "Reduction of motion artifact in pulse oximetry by smoothed pseudo wigner-ville distribution," *Journal of NeuroEngineering and Rehabilitation*, vol. 2, no. 1, p. 3, 2005.

[5] M. Nurmi, "Dynamic control algorithm for an analog front end in a wearable optical heart rate monitoring device; dynaaminen säätöalgoritmi fotopletysmografiaan perustuvalle rannesykemittarille," G2 Pro gradu, diplomityö, 2016-06-13. [Online]. Available: http://urn.fi/URN:NBN:fi:aalto-201606172477

[6] M. Lemay, M. Bertchi, J. Sola, P. Renevey, J. Parak, and I. Korhonen, "Application of optical heart rate monitoring," in *Wearable Sensors: Fundamentals, Implementation and Applications*. Elsevier, 2014, pp. 105–129.

[7] T. Tamura, Y. Maeda, M. Sekine, and M. Yoshida, "Wearable photoplethysmographic sensors—past and present," *Electronics*, vol. 3, no. 2, pp. 282–302, 2014.

[8] Y. Maeda, M. Sekine, T. Tamura, A. Moriya, T. Suzuki, and K. Kameyama, "Comparison of reflected green light and infrared photoplethysmography," in *Engineering in Medicine and Biology Society, 2008. EMBS 2008. 30th Annual International Conference of the IEEE*. IEEE, 2008, pp. 2270–2272.

[9] P. G. Montgomery, D. J. Green, N. Etxebarria, D. B. Pyne, P. U. Saunders, and C. L. Minahan, "Validation of heart rate monitor-based predictions of oxygen uptake and energy expenditure," *The Journal of Strength & Conditioning Research*, vol. 23, no. 5, pp. 1489–1495, 2009.

[10] A. Uusitalo, T. Mets, K. Martinmäki, S. Mauno, U. Kinnunen, and H. Rusko, "Heart rate variability related to effort at work," *Applied Ergonomics*, vol. 42, no. 6, pp. 830–838, 2011.

[11] J. Achten and A. E. Jeukendrup, "Heart rate monitoring," *Sports medicine*, vol. 33, no. 7, pp. 517–538, 2003.

[12] A. Ahtinen, J. Mantyjarvi, and J. Hakkila, "Using heart rate monitors for personal wellness-the user experience perspective," in *Engineering in Medicine and Biology Society, 2008. EMBS 2008. 30th Annual International Conference of the IEEE*. IEEE, 2008, pp. 1591–1597.

[13] R. M. Laukkanen and P. K. Virtanen, "Heart rate monitors: state of the art," *Journal of sports sciences*, vol. 16, no. sup1, pp. 3–7, 1998.

[14] R. Delgado-Gonzalo, J. Parak, A. Tarniceriu, P. Renevey, M. Bertschi, and I. Korhonen, "Evaluation of accuracy and reliability of pulseon optical heart rate monitoring device," in *Engineering in Medicine and Biology Society (EMBC), 2015 37th Annual International Conference of the IEEE*. IEEE, 2015, pp. 430–433.

[15] Y. Mendelson and B. D. Ochs, "Noninvasive pulse oximetry utilizing skin reflectance photoplethysmography," *IEEE Transactions on Biomedical Engineering*, vol. 35, no. 10, pp. 798–805, 1988.

[16] F.-H. Huang, P.-J. Yuan, K.-P. Lin, H.-H. Chang, and C.-L. Tsai, "Analysis of reflectance photoplethysmograph sensors," *World Academy of Science, Engineering and Technology*, vol. 59, no. 241, pp. 1266–1269, 2011.

[17] S. Rhee, B.-H. Yang, and H. H. Asada, "Artifact-resistant power-efficient design of finger-ring plethysmographic sensors," *IEEE transactions on biomedical engineering*, vol. 48, no. 7, pp. 795–805, 2001.

[18] E. S. Winokur, "Single-site, noninvasive, blood pressure measurements at the ear using ballistocardiogram (bcg), and photoplethysmogram (ppg), and a low-power, reflectance-mode ppg soc," Ph.D. dissertation, Massachusetts Institute of Technology, 2014.

[19] O. opto semiconductors, "High-speed switching of ir-leds (part i).application note," 2014.

[20] H. Haugan, S. Elhamri, F. Szmulowicz, B. Ullrich, G. Brown, and W. Mitchel, "Study of residual background carriers in midinfrared in as/ ga sb superlattices for uncooled detector operation," *Applied Physics Letters*, vol. 92, no. 7, p. 071102, 2008.

[21] J. May, "Investigation of fontanelle photoplethysmographs and oxygen saturations in intensive care neonates and infants utilising miniature photometric sensors," Ph.D. dissertation, City University London, 2013.

[22] Zen-in. Transimpedance amplifier, a schematic illustration. [Online]. Available: https://en.wikipedia.org/wiki/File:TIA_simple.svg

[23] "Adpd153ggri integrated optical module with ambient light rejection and four leds."

[24] "Optical sensor comparison journal=Technical report organization=CSEM, Neuchatel,Switzerland year=2015."

[25] D. M. Tavakoli, "An analog vlsi front end for pulse oximetry." 2006.

[26] K. N. Glaros and E. M. Drakakis, "A sub-mw fully-integrated pulse oximeter front-end," *IEEE transactions on biomedical circuits and systems*, vol. 7, no. 3, pp. 363–375, 2013.

[27] J. A. Patterson and G.-Z. Yang, "Dual-mode additive noise rejection in wearable photoplethysmography," in *Wearable and Implantable Body Sensor Networks (BSN), 2012 Ninth International Conference on*. IEEE, 2012, pp. 97–102.

[28] E. S. Winokur, T. O'Dwyer, and C. G. Sodini, "A low-power, dual-wavelength photoplethysmogram (ppg) soc with static and time-varying interferer removal," *IEEE transactions on biomedical circuits and systems*, vol. 9, no. 4, pp. 581–589, 2015.

[29] A. Al-Ali, M. K. Diab, M. E. Kiani, R. J. Kopotic, and D. Tobler, "Stereo pulse oximeter," Dec. 25 2001, uS Patent 6,334,065.

[30] P. W. Cheung, K. F. Gauglitz, S. W. Hunsaker, S. J. Prosser, D. O. Wagner, and R. E. Smith, "Apparatus for the automatic calibration of signals employed in oximetry," Nov. 9 1993, uS Patent 5,259,381.

[31] *PulseOn white label OHR device data sheet*, PulseOn Oy, 08 2017.

[32] *AFE4404 Ultra-Small, Integrated AFE for Wearable, Optical, Heart-Rate Monitoring and Bio-Sensing*, Texas Instruments, 12 2016.

[33] M. Grusin. Serial peripheral interface (spi). [Online]. Available: https://learn.sparkfun.com/tutorials/serial-peripheral-interface-spi

[34] J. D'Orazio, S. Jarrett, A. Amaro-Ortiz, and T. Scott, "Uv radiation and the skin," *International journal of molecular sciences*, vol. 14, no. 6, pp. 12 222–12 248, 2013.

[35] G. Company. Heart rate monitor instructions. [Online]. Available: http://static.garmin.com/pumac/HRM3_Instructions_ML12.pdf

[36] T. Tamura, Y. Maeda, M. Sekine, and M. Yoshida, "Wearable photoplethysmographic sensors—past and present," *Electronics*, vol. 3, no. 2, pp. 282–302, 2014. [Online]. Available: http://www.mdpi.com/2079-9292/3/2/282

[37] B. A. Fallow, T. Tarumi, and H. Tanaka, "Influence of skin type and wavelength on light wave reflectance," *Journal of clinical monitoring and computing*, vol. 27, no. 3, pp. 313–317, 2013.

A Sports_protocol

Activity	Start time (min)	End time (min)	Duration (min)
Rest sitting (no motion)	0:00	1:00	1:00
Warm up with ergocycle	1:00	4:00	3:00
Rest standing / transition	4:00	5:00	1:00
Walking 3 km/h on treadmill, 0 % inclination	5:00	8:00	3:00
Walking 3 km/h on treadmill, 5 % inclination	8:00	11:00	3:00
Walking 3 km/h on treadmill, 10 % inclination	11:00	14:00	3:00
Walking 5 km/h on treadmill, 0 % inclination	14:00	17:00	3:00
Walking 5 km/h on treadmill, 5 % inclination	17:00	20:00	3:00
Walking 5 km/h on treadmill, 10 % inclination	20:00	23:00	3:00
Running 9 km/h on treadmill, 0 % inclination	23:00	26:00:00	3:00
Running 11 km/h on treadmill, 0 % inclination	26:00:00	29:00:00	3:00
Rest sitting / transition	29:00:00	30:00:00	1:00
Ergocycle 50 W, 60 rpm cadence	30:00:00	33:00:00	3:00
Ergocycle 75-100 W, 90 rpm cadence*	33:00:00	36:00:00	3:00
Rest sitting / transition	36:00:00	37:00:00	1:00
Rowing	37:00:00	39:00:00	2:00
Rest standing	39:00:00	40:00:00	1:00
Push ups	40:00:00	41:00:00	1:00
Rest standing	41:00:00	42:00:00	1:00
”Haara-perushyppelyä”	42:00:00	43:00:00	1:00
Rest sitting	43:00:00	45:00:00	2:00